

TECHNOTE



U.S. Department of Transportation
Federal Highway Administration

Turner-Fairbank
Highway Research Center

Research, Development,
and Technology
Turner-Fairbank Highway
Research Center
6300 Georgetown Pike
McLean, VA 22101-2296
<https://highways.dot.gov/research>

Portland Limestone Cement Variability

FHWA Publication No.: FHWA-HRT-25-116

FHWA Contact: Michelle A. Cooper (ORCID: 0000-0001-8112-693X),
HRDI-10, michelle.cooper@dot.gov

Authors:

Payam Hosseini, GENEX Systems,
(ORCID: 0000-0001-5670-577X), payam.hosseini.ctr@dot.gov

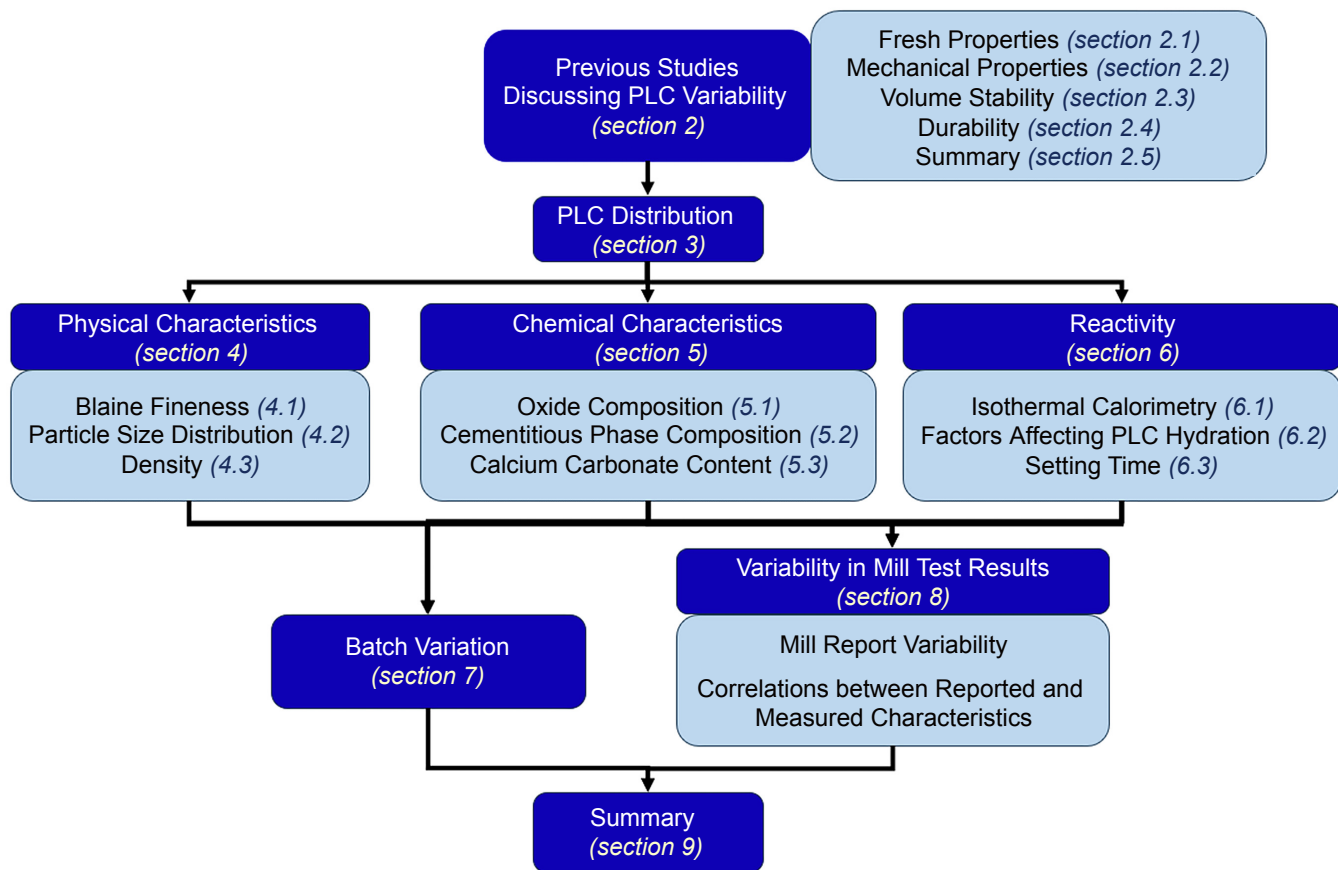
Michelle A. Cooper, FHWA (ORCID: 0000-0001-8112-693X),
michelle.cooper@dot.gov

Scott Muzenski, GENEX Systems,
(ORCID: 0000-0003-1694-0278), scott.muzenski.ctr@dot.gov

1. INTRODUCTION

Portland limestone cement (PLC), also known as Type IL, is a blended hydraulic cement that contains 5–15 percent (by weight) limestone (either blended fines or interground with clinker) to reduce the clinker content.⁽¹⁾ ASTM International (ASTM) C595⁽²⁾ and American Association of State Highway and Transportation Officials (AASHTO) M 240⁽³⁾ provide specifications for PLC characteristics. With PLC's recent adoption and expansion throughout the United States to replace ordinary portland cement (OPC), large-scale production of PLC is now widespread. More than half of the cement consumed in the United States is PLC rather than OPC⁽⁴⁾, making PLC the most common type of cement in the United States.⁽⁵⁾ While considerable research has been conducted on PLC, much of that work was performed using a few PLCs from different sources, which do not provide insight into the effect of variations in the characteristics of PLC on the performance of the final products, such as concrete mixtures. Considering the variability in performance of PLCs reported in field applications⁽⁶⁾, the opportunity now exists for PLC products created at production scale from varying cement plants and with varying limestone contents to be characterized. Cements are typically distributed across State lines to supply projects. Therefore, understanding the range of characteristics and behaviors that different PLC products may exhibit is important to consistent concrete production. This TechNote aims to provide State highway agencies and contractors with information on the variability of PLC throughout the United States. A better understanding of variability in PLCs' physical and chemical characteristics and its effect on PLC behavior can help enhance PLC performance in the field. This TechNote does not aim to compare PLC with OPC variability or performance and is intended to provide a general perspective on differences in PLC characteristics across the country. The discussion of Type IL cement variability in this document does not, in any way, suggest that there is no variability in Type I/II cement. Also, the changes in concrete performance resulting from variability in Type IL cement does not mean Type I/II cement variability does not cause similar changes in concrete performance. Figure 1 displays a graphical abstract of the document.

Figure 1. Diagram. Graphical abstract illustrating the structure of this TechNote.



Source: Federal Highway Administration (FHWA).

2. PREVIOUS STUDIES DISCUSSING PLC VARIABILITY

This section examines how the variability in PLC characteristics can impact key performance aspects of concrete, including its fresh state, mechanical properties, volume stability, and durability, based on previous studies. Note that the incorporation of supplementary cementitious materials (SCMs) can influence the performance of PLC differently compared to OPC systems^(7,8,9,10), which is not the focus of this work. Further details on PLC characteristics and performance, not specifically discussing variability of PLC, can be found in previous studies.^(11,12)

2.1 Fresh Properties

The use of PLC influences the workability and bleeding of concrete due to its finer particle sizes compared to OPC.^(1,7,13) This effect is more pronounced in concretes with a lower water-to-cementitious materials ratio⁽⁷⁾,

necessitating the use of more water-reducing admixture to achieve a similar slump range. As the fineness of the PLC increases, workability (slump according to ASTM C143⁽¹⁴⁾) is reduced in concrete mixtures.⁽¹³⁾

Generally, higher fineness leads to faster hydration, which in turn decreases the setting time due to the larger surface area of clinker particles available for reaction and/or the increased number of nucleation sites on limestone particles.⁽⁷⁾ However, a study by Hansen et al.⁽¹³⁾ indicated that there is no specific trend in the effect of PLC fineness (from 467 m²/kg to 568 m²/kg) on the initial setting time for concrete mixtures. Moreover, in PLC paste systems, this trend can be altered by the dosage of sulfate (SO₄²⁻) source added during grinding to control set and aluminate (tricalcium aluminate or C₃A) content present in the clinker particles.⁽⁷⁾ Additionally, the calcium carbonate (CaCO₃) content of the limestone exhibited an inverse relationship with both the initial and final setting times

in PLC paste systems; however, its effect was more pronounced on the final setting time.⁽⁷⁾

Using the same dosage of air entrainer, air-entrained concrete with PLC exhibited lower air content than those with OPC. This difference in behavior was attributed to the finer particle size and higher surface area of PLC.⁽⁷⁾

2.2 Mechanical Properties

Increasing PLC fineness generally leads to an increase in the early-age (1 to 7 d) and midterm (28 and 56 d) compressive strength of concrete mixtures, as shown by Hansen et al.⁽¹³⁾, regardless of the type of coarse aggregate.

Kurtis et al.⁽⁷⁾ indicated that PLC fineness has a significant effect on early-age (1-d) compressive strength, but a lower effect on long-term (1 yr) compressive strength for concrete mixtures designed for different 28-d compressive strengths (3,000, 3,500, and 5,000 psi).¹ Furthermore, regardless of concrete strength class, higher calcite content and therefore higher limestone contents resulted in higher compressive strengths; however, this effect diminished after long-term curing (1 yr).⁽⁷⁾ In addition to fineness and calcite content, PLC's chemical composition contributes to compressive strength development.⁽⁷⁾ When compared to concrete made with OPC, concretes with PLC showed varied effects (higher and lower) on the compressive strength of concrete across different strength classes, with a greater impact observed on concrete with higher compressive strength.⁽⁷⁾ For example, in the 3,000 psi compressive strength class, PLC mixtures exhibited reduced long-term compressive strength compared to their OPC counterparts, despite having higher early-age compressive strength, regardless of PLC fineness. However, in the 5,000 psi compressive strength class, finer PLC demonstrated higher compressive strength at all ages, while coarser PLC showed lower compressive strength at all ages compared to their OPC counterparts.⁽⁷⁾ Furthermore, the positive effects of PLC fineness and calcite content on compressive strength were more pronounced in concretes with higher compressive strength classes (e.g., 3,000 psi versus 5,000 psi), regardless of the age of the concrete samples.

According to Barrett et al.⁽¹⁵⁾, the compressive strength of concrete mixtures with three PLCs and various water-to-cement ratios (w/c) (0.38, 0.42, and 0.46) cured for up to 1 yr were within ± 10 percent of the OPC system with the same volume replacement for cement. At 28 d, all three types of tested PLCs resulted in an average increase of 1.5 percent in compressive strength, with a maximum decrease of 6 percent at the various w/c ratios

utilized in their study. Regardless of PLC characteristics, the compressive strength of concrete made with PLC was comparable to that of concrete made with OPC across various w/c ratios.

Higher fineness (finer particle size) of PLC resulted in increased splitting tensile strength at 28 d.⁽⁷⁾ However, no correlation was observed between the 28-d splitting tensile strength and calcite content.⁽⁷⁾ Additionally, statistical analysis revealed that, regardless of the concrete's compressive strength class, the source of PLC (various cement producers) had a greater impact on splitting tensile strength than the cement type (PLC versus OPC).⁽¹⁵⁾

Concrete mixtures made with various PLCs and w/c ratios (0.38, 0.42, and 0.46) showed negligible differences (with a maximum of 7-percent reduction) in the modulus of elasticity (MOE) compared to concrete mixtures using the companion OPC system at up to 1 yr of curing.⁽¹⁵⁾ In general, the MOE at 28 d does not follow the trends of compressive strength in concrete mixtures made with PLC⁽⁷⁾; however, due to the limited number of PLCs tested (two), additional research may be necessary. For instance, increasing the calcite content in PLC reduced the 28-d MOE for concretes with compressive strength classes of 3,000 and 5,000 psi. However, for concretes with a compressive strength class of 3,500 psi, the 28-d MOE increased with higher calcite content. Furthermore, no correlation was observed between the PLC fineness (in terms of average particle size) and its 28-d MOE.

2.3 Volume Stability

Previous studies have shown that the effect of PLC on the volume stability of cement-based materials varies depending on PLC's physical (fineness) and chemical (clinker phase composition and percentage) characteristics.^(7,15) However, for OPC and PLC with the same source of clinker, finer cement results in higher volume changes in cement paste (autogenous and chemical).⁽⁷⁾ Moreover, PLC exhibits varied effects on early and long-term drying shrinkage of concrete samples depending on their compressive strength class⁽⁷⁾ and therefore on the mixture design. For concrete with a lower strength level (3,000 psi), there was no statistically significant difference between PLC and OPC for early-age (7 d) drying shrinkage, while finer PLC reduced long-term (1 yr) drying shrinkage.⁽⁷⁾ Conversely, for concrete samples with a higher compressive strength class (5,000 psi), the opposite trend was observed.⁽⁷⁾ For concretes with a compressive strength class of 3,500 psi, increasing the calcite content in PLC and using finer PLC resulted in greater drying shrinkage, both at early (7 d)

¹Compressive strength was adjusted by varying w/c ratio. Strength classes of 3,000, 3,500, and 5,000 psi were achieved with w/c ratios of 0.490, 0.445, and 0.320, respectively.

and long-term (1 yr) stages.⁽⁷⁾ Moreover, PLC concrete with a higher compressive strength class (5,000 psi) exhibited lower drying shrinkage than concrete with a lower compressive strength level (3,500 psi).⁽⁷⁾ These conflicting trends indicate that concrete mixture design proportions (such as paste content) may have a greater influence on volume stability than cement characteristics.

Barrett et al.⁽¹⁵⁾ demonstrated that the restrained shrinkage behavior of mortar mixtures with PLC is similar to that of the control OPC if the PLC is ground to levels required to achieve comparable compressive strength to the OPC system. However, if the PLC is ground finer (more than 30 percent finer than OPC), increased early-age shrinkage is observed due to higher residual stress development and a reduction in the remaining stress capacity of the matrix.⁽¹⁵⁾

2.4 Durability

Kurtis et al.⁽⁷⁾ indicated that there are no changes in permeability classification based on total charge passed (via the rapid chloride penetration test (RCPT))^(16,17) between concretes with OPC and PLC of the same clinker composition from various sources (i.e., different cement producers). However, no specific correlation between electrical surface resistivity (SR) and the fineness or limestone dosage of PLC was observed, suggesting that other factors, such as changes in pore solution chemistry due to the utilization of limestone in PLC, may play a role.⁽⁷⁾ Hansen et al. also found no statistically significant changes in the SR of concrete mixtures with varying PLC fineness.⁽¹³⁾

Barrett et al.⁽¹⁵⁾ found that concrete mixtures with PLC had slightly higher volumes of permeable voids (up to 10 percent) after 90 d of curing compared to concrete mixtures made with OPC systems. Additionally, depending on the characteristics of the PLC, especially its fineness, the chloride diffusion coefficient of concrete samples increased by 2 to 30 percent, with finer PLC showing a smaller increase in the chloride diffusion coefficient compared to concretes made with their OPC counterparts.⁽¹⁵⁾

Although air-entrained concrete mixtures with PLC showed lower air content, their freeze-thaw resistance was similar to that of concrete made with OPC.⁽⁷⁾ In addition, mortar samples made with PLC from various clinker

sources² exhibited reduced expansion in accelerated alkali-silica reactivity test⁽¹⁸⁾ results, which the authors of the study attributed to the reduced alkali content in cement due to limestone replacement.⁽¹⁰⁾

2.5 Summary

Previous studies on the effect of PLC variability on concrete performance indicate that increased PLC fineness reduces workability. Additionally, higher PLC fineness and/or calcite content shortens PLC paste setting times.

Regarding mechanical performance, increasing PLC fineness and/or calcite content generally enhances compressive strength at almost all curing ages. However, PLC fineness has a greater effect than calcite content on splitting tensile strength. While calcite content has little impact on 28-d splitting tensile strength, higher PLC fineness leads to an increase. No clear trend is observed in the MOE with variations in PLC fineness and calcite content.

In terms of volume stability, higher PLC fineness decreases resistance to restrained shrinkage in PLC mortar, while its effect on concrete drying shrinkage depends on the cement and paste contents used to attain the compressive strength class. Higher calcite content in PLC leads to greater drying shrinkage in PLC concrete.

Regarding durability, higher PLC fineness reduces total charge passed through concrete during RCPT but has minimal impact on SR. Calcite content does not exhibit a consistent influence on concrete SR.

Table 1 summarizes the impact of variability in PLC characteristics on concrete properties.

3. PLC DISTRIBUTION

This study used 18 PLC samples from 13 different cement plants in 9 States across the United States between 2022 and 2025 to represent variability in commercially available PLC products resulting from different geology, raw materials, production methods, grinding aids, etc. Figure 2 shows a distribution of plants by State from which PLC samples were collected.

²Clinkers that were used to produce various OPC types (II, II/V, and V).

Table 1. Summary of the effects of variability in PLC characteristics on performance of concrete materials based on other studies. (See references 7, 10, 13, and 15.)

PLC Characteristics	Concrete Properties								RCPT	SR
	Workability ♣	Paste Setting Time	Compressive Strength	28-Day Splitting Tensile Strength	28-Day MOE	Drying Shrinkage	Restrained Shrinkage (Equivalent Mortar Mixture)			
Fineness ↑	↓	↓	Early age ↑ Midterm ↑ Long term ↑*	↑	~	Depends on strength class of concrete	↑	↓	~	
Calcite ↑	NA	↓	Early age ↑ Midterm ↑ Long term ↑*	~	ME	↑**	NA	NA	ME	

♣ = Measured by slump test according to ASTM C143.⁽¹⁴⁾

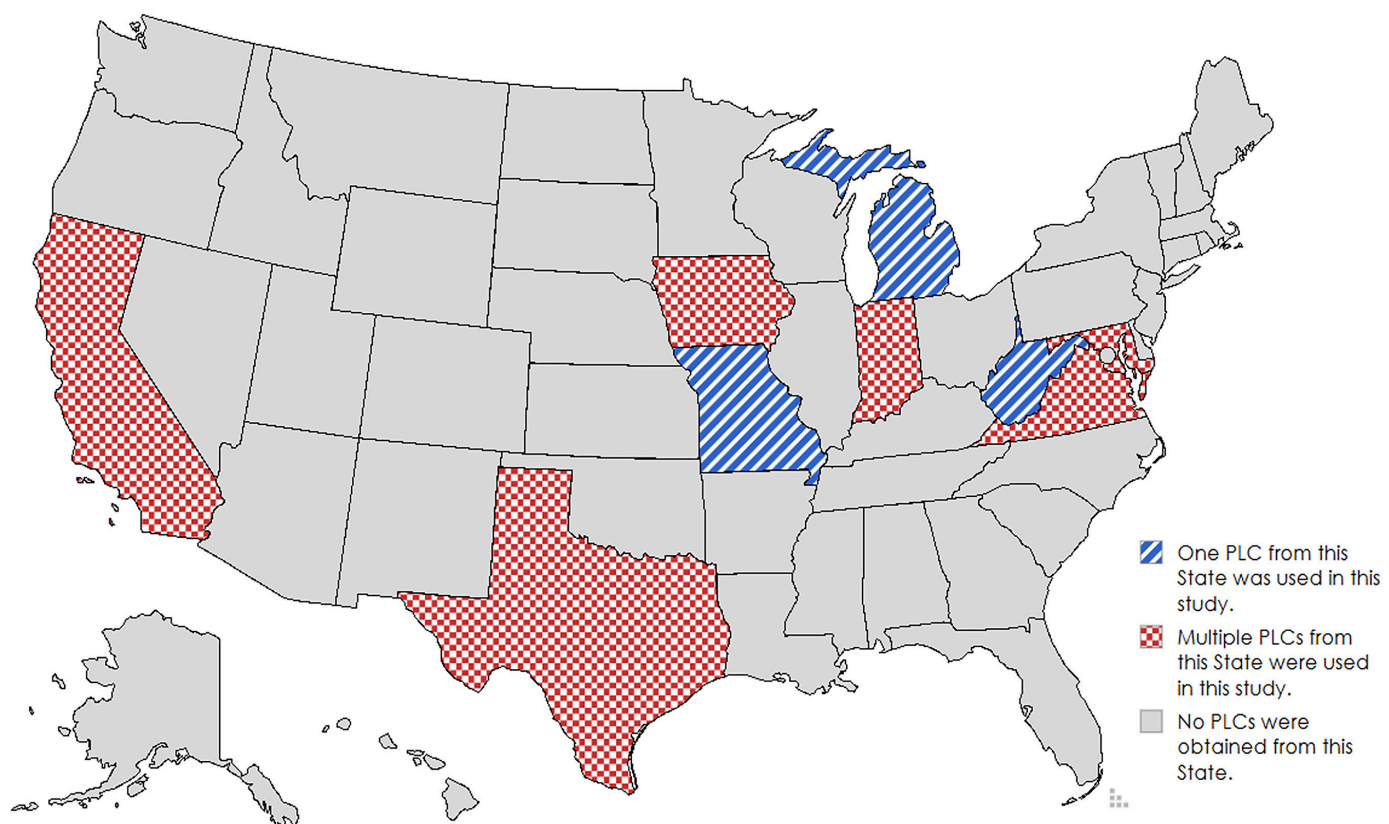
* = Significant for concretes of higher compressive strength class.

~ = No effect.

** = Based on limited data.

NA = The information is not available; ME = There is a mixed effect or no consistent relationship.

Figure 2. Image. Map of samples obtained from PLC plants.



Map by MapChart is licensed under CC BY-SA 4.0 and was modified by FHWA.⁽¹⁹⁾ Modifications by FHWA to show the sources of cement in this research project.

4. PHYSICAL CHARACTERISTICS

4.1 Blaine Fineness

Blaine fineness is an indirect measure of the specific surface area of cement particles, which is directly related to their reactivity. The fineness, therefore, significantly influences fresh (workability) and hardened (mechanical and durability) properties of cementitious materials.⁽²⁰⁾ However, in a survey on 45 commercially available PLCs in the United States in 2022⁽⁵⁾, it was shown that increasing the Blaine fineness slightly increased compressive strength of PLC mortar cubes (according to ASTM C109⁽²¹⁾) up to 7 d and its effect diminished at 28 d.

Blaine fineness measurements were performed on the 18 PLC samples according to ASTM C204⁽²²⁾, and AASHTO T 153.⁽²³⁾ Figure 3 shows the variation of Blaine fineness for the tested PLCs. As seen in figure 3, half of the samples have a Blaine fineness between 405.4 m²/kg and 413.7 m²/kg, with the average Blaine fineness for the tested PLCs being 414.2 m²/kg. In a survey on 45 commercially available PLCs in the United States in 2022, the mean value for Blaine fineness was reported as 465.0±39.1 m²/kg.

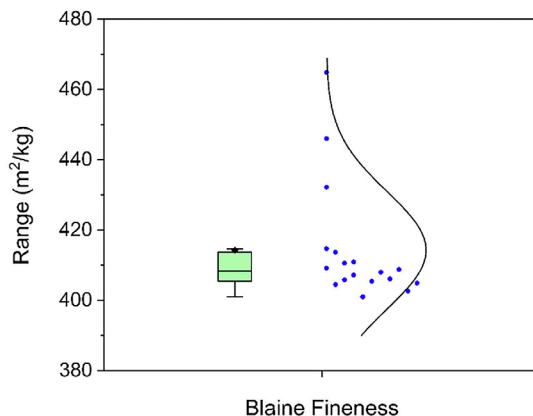
4.2 Particle Size Distribution

Blaine fineness measurement remains the industry standard for mill test reports. However, due to its reliability issues with particles having high specific surface areas, such as SCMs⁽²⁴⁾, the industry is shifting toward particle size distribution measurements using laser diffraction and sieve analysis, particularly for blended cements. Since PLC contains fine limestone particles, the Blaine fineness test may not accurately indicate its fineness. Additionally, the prehydration of a small portion of PLC may contribute to greater variability in Blaine fineness measurement data.

The particle size distribution of a cement sample affects its performance and is directly related to its specific surface area. Particle size distribution for PLC samples was measured using a laser diffraction particle size analyzer. Figure 4 shows the results.

In figure 4, $D_{(10)}$, $D_{(50)}$, and $D_{(90)}$ represent the particle sizes at which 10, 50, and 90 percent of the PLC sample volume is smaller, respectively. In addition, $D_{(average)}$ indicates the volume mean diameter for all PLC samples. The average $D_{(10)}$, $D_{(50)}$, $D_{(90)}$, and $D_{(average)}$ values for the tested PLCs are 1.6 µm, 11.6 µm, 36.0 µm, and 15.7 µm, respectively. $D_{(90)}$ exhibits greater variability than $D_{(50)}$, which, in turn, shows larger variations than $D_{(10)}$. This result indicates that the finer portion of the PLC samples had narrower variability. In other words, larger particles increase the variability in the particle size distribution of PLCs. However, this result also suggests that factors such as the hardness and size of PLC ingredients (e.g., clinker,

Figure 3. Distribution and range of Blaine fineness among PLC samples. A normal distribution was shown for comparison purposes. (♦ shows the average value for the data.)



Source: FHWA.

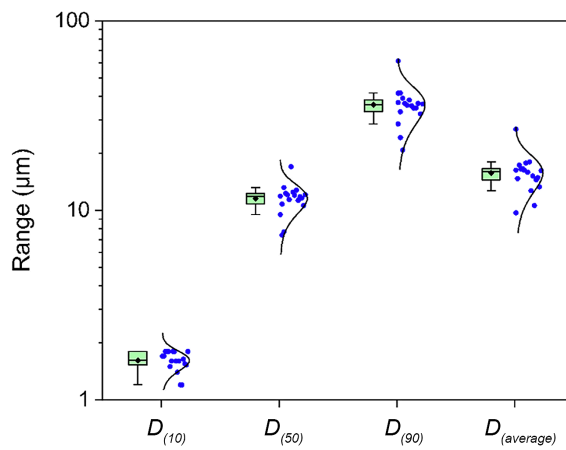
limestone, and calcium sulfates), application of grinding aids, and the current milling technology and duration used in cement plants, have minimal impact on the variability of the finest portion of PLCs.

As shown in table 1, PLC fineness is a key factor influencing cement performance in concrete materials. While most commercially available PLCs in this study exhibited minimal variability in particle size distributions (figure 4 and figure 5), greater variability in the coarser fractions was observed, which can affect PLC behavior, especially during early ages where the rate of dissolution of cement particles is critical. Furthermore, the variability in the largest particle fraction may be due to the prehydration of a small portion of PLCs during handling, as evidenced by the presence of calcium hydroxide in PLC samples discussed in the cementitious phase composition section of this TechNote.

Figure 5 shows the particle size distribution for the tested PLCs. For all PLCs tested, there are three humps indicating increased volume percentages in the particle size distributions, which can be categorized within the 10–50 µm, 1–10 µm, and 0.1–1 µm particle size ranges, referred to as hump 1, hump 2, and hump 3, respectively. Most PLC particles are within the 10–50 µm size range, as reflected with the $D_{(average)}$ value of 15.7 µm.

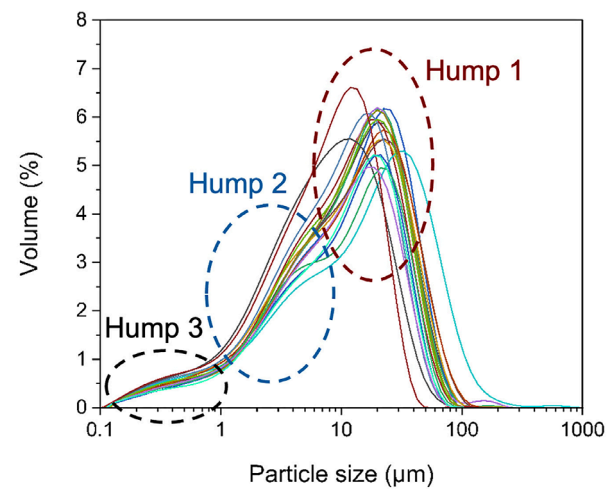
Figure 6 illustrates the relationships between various particle size distribution indicators and Blaine fineness for PLC samples. The results suggest no clear correlation, indicating that Blaine fineness may not be a suitable test method for PLCs, which is consistent with results seen regarding fineness testing of SCMs.⁽²⁴⁾

Figure 4. Graph. Distribution and range of particle size distribution indicators for PLC samples. A normal distribution was shown for comparison purposes. (♦ shows the average value for the data.)



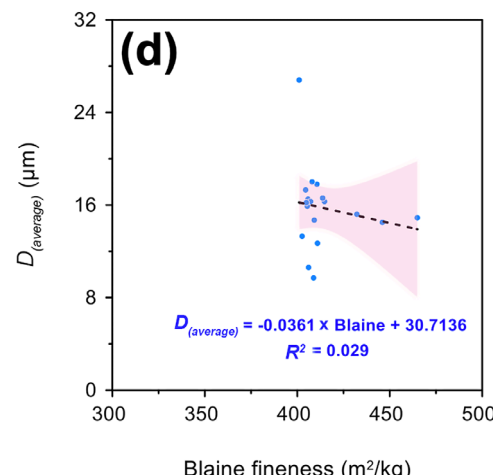
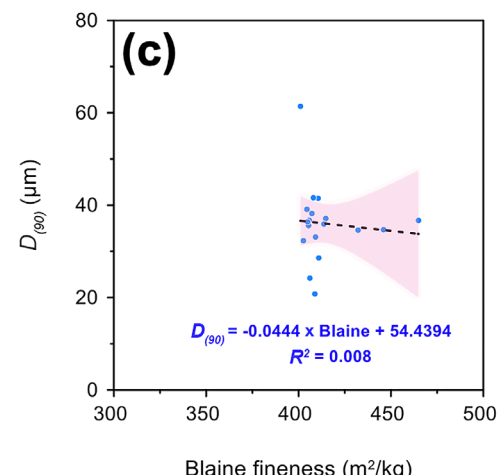
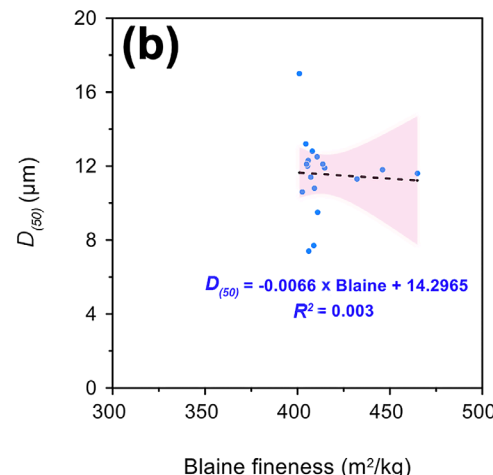
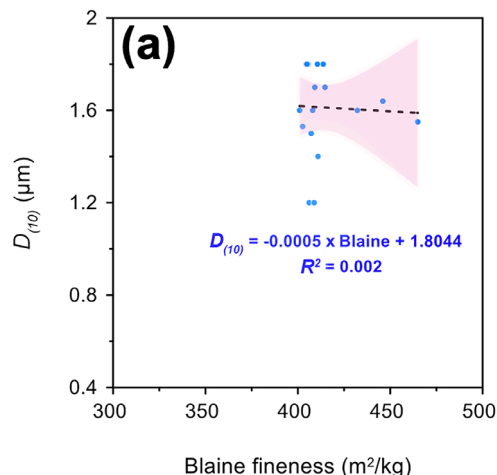
Source: FHWA.

Figure 5. Graph. Particle size distribution for the tested PLC samples.



Source: FHWA.

Figure 6. Graph. Relationships between particle size distribution indicators (with (a) showing $D_{(10)}$, (b) showing $D_{(50)}$, (c) showing $D_{(90)}$, and (d) showing $D_{(average)}$) and Blaine fineness for PLCs, where the shaded regions demonstrate 95-percent confidence bands, and the dashed lines show the data trends.



Source: FHWA.

4.3 Density

Limestone has a lower density (2.60–2.70 g/cm³) than ground portland cement clinker (3.15–3.30 g/cm³), resulting in a lower density for PLC compared to OPC due to the higher limestone content in PLC. Thus, density measurements can serve as a quality-control indicator because excessively low or high density may suggest a product with a limestone content outside the 5–15 percent by weight range.

Density measurements on PLC samples, shown in figure 7, were conducted following a modified version of ASTM C188⁽²⁵⁾, which uses isopropanol instead of kerosene to conduct the measurements. This modification to the test method has been demonstrated to have negligible impacts on the results, having only a 0.3 percent difference from kerosene measurements on average.⁽²⁶⁾ Based on the results obtained, the average density for the tested PLCs is 3.07 g/cm³, with half of the samples within a density range of 3.06 to 3.08 g/cm³.

5. CHEMICAL CHARACTERISTICS

5.1 Oxide Composition

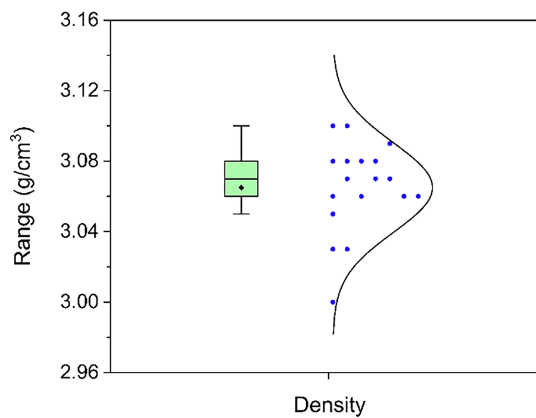
The oxide composition of OPC provides valuable information because it allows for the use of Bogue's formulations (as per ASTM C150⁽²⁷⁾) to accurately estimate phase composition. However, Bogue's formulations are not applicable to PLC due to the impurities introduced by the incorporated limestone.⁽⁷⁾

Oxide composition of PLC samples was obtained through wavelength dispersive X-ray fluorescence spectrometry based on ASTM C114.⁽²⁸⁾ Figure 8 presents oxide composition and loss on ignition (LOI) for PLC samples. The average weight percentage for the major oxides, including aluminum oxide (Al₂O₃), calcium oxide (CaO), silicon dioxide (SiO₂), iron oxide (Fe₂O₃), sodium oxide (Na₂O), potassium oxide (K₂O), magnesium oxide (MgO), and sulfur trioxide (SO₃) in the tested PLCs is 4.58, 61.93, 19.01, 2.79, 0.14, 0.49, 2.39, and 2.94 percent, respectively. In addition, the average LOI for the tested PLCs is 5.11 percent.

For comparison perspectives, in a recent survey on 45 commercially available PLCs in the United States in 2022⁽⁵⁾, the mean weight percentage for MgO, SO₃, and LOI was reported as 2.07, 3.12, and 5.44 percent, respectively.

According to ASTM C595⁽²⁾ and AASHTO M 240⁽³⁾, the LOI content should be limited to 10 percent by weight, a criterion met by all tested PLCs. Additionally, the

Figure 7. Graph. Distribution and range of density for PLC samples. A normal distribution was shown for comparison purposes. (♦ shows the average value for the data.)



Source: FHWA.

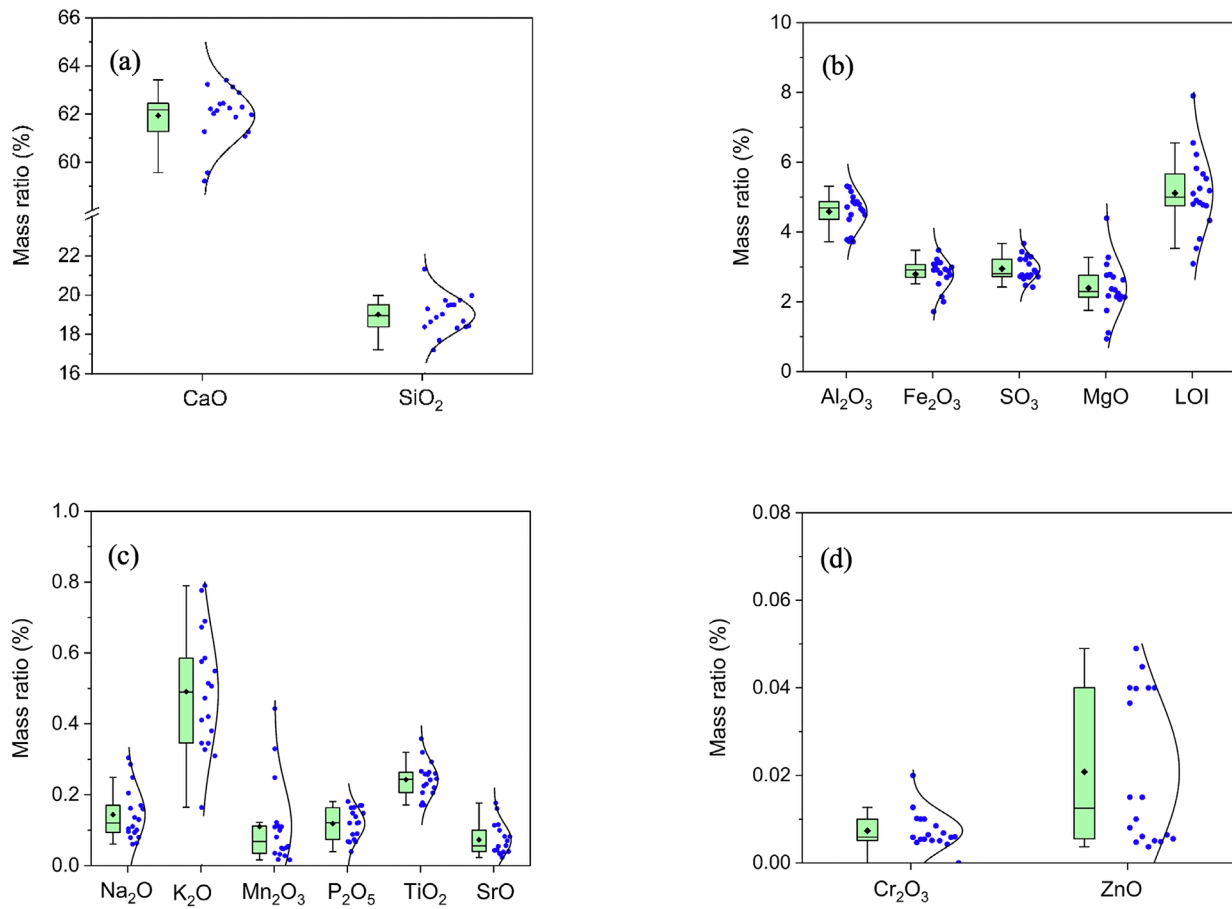
SO₃ content must be limited to 3.0 percent by weight; however, this threshold was exceeded by 7 out of 18 PLCs (39 percent of the PLCs tested in this study) with a maximum of 3.67 percent by weight. Nevertheless, mortar expansion measurements for these samples, as reported in their technical data sheets and conducted by the PLC manufacturers in accordance with ASTM C1038⁽²⁹⁾, were below 0.020 percent, meeting the specifications of ASTM C595.⁽²⁾

5.2 Cementitious Phase Composition

Cementitious phases are major factors in determining the reactivity and, thus, the fresh and hardened performance of cement. X-ray powder diffraction data are used to quantify crystalline phases within cementitious materials through quantitative X-ray powder diffraction (QXRD) using the Rietveld method.⁽³⁰⁾ As previously mentioned, although Bogue's formulations are employed to reasonably estimate the quantities of cementitious phases within OPC⁽²⁷⁾, this method does not work for PLC due to the limestone.⁽⁷⁾ Therefore, QXRD can be practically employed to obtain the mass ratio of cementitious phases in PLC.

The QXRD method was validated using the National Institute of Standards and Technology's Standard Reference Material (SRM[®]) clinker 2686b in accordance with ASTM C1365.⁽³¹⁾ SRM 2686b was milled and passed through a 45 µm (325 mesh) sieve. Figure 9 presents the QXRD results. According to the QXRD analysis, the major cementitious phases in the PLC samples were alite (C₃S), CaCO₃, C₃A, ferrite (C₄AF), and belite (C₂S), with average mass ratios of 55.5, 10.5, 6.4, 10.3, and 7.7 percent, respectively.

Figure 8. Graph. Mass ratio distribution of oxides and LOI of the PLCs. A normal distribution was shown for comparison purposes. (♦ shows the average value for the data.)



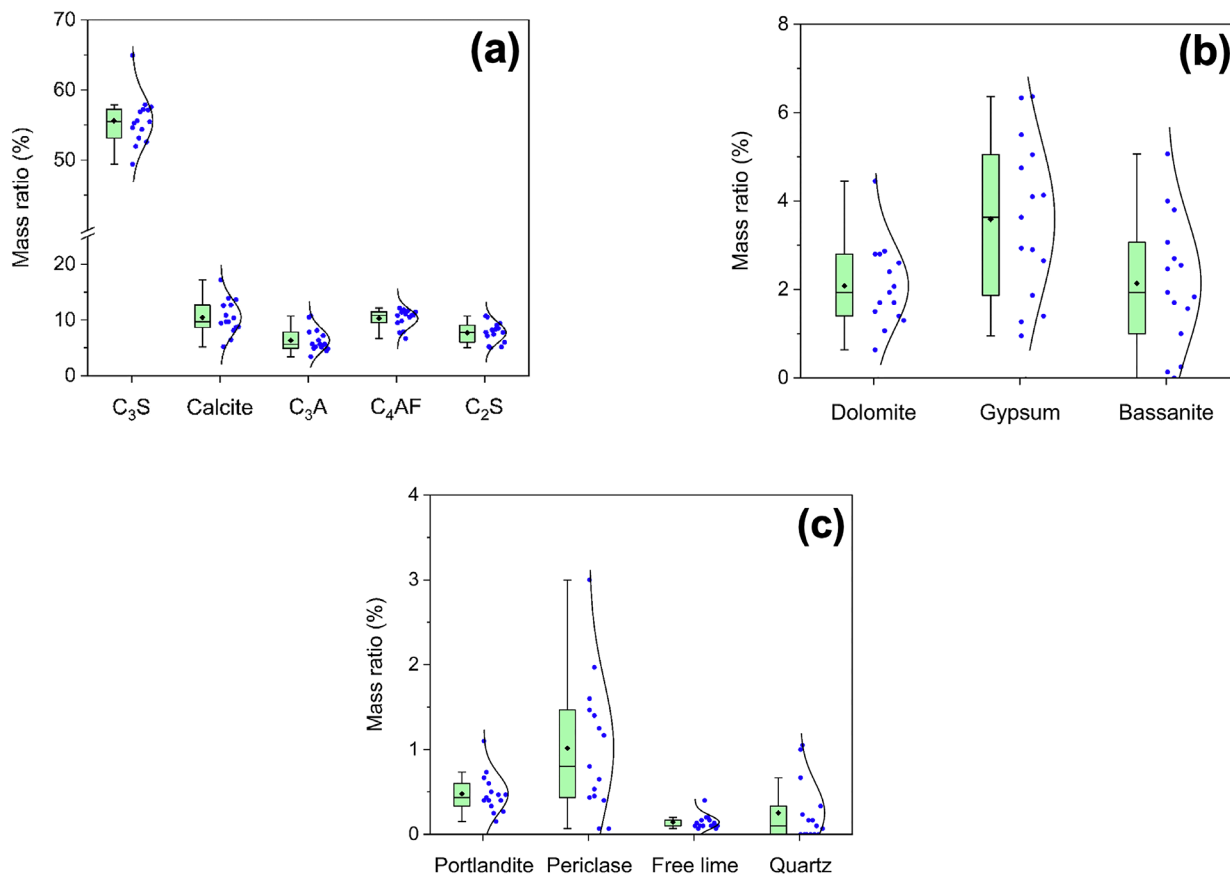
Source: FHWA.

Cr_2O_3 = Chromium (III) oxide.

The calcium silicate phases, which primarily contribute to the early and later-age mechanical and durability properties of concrete due to the production of calcium-silicate-hydrate (C-S-H) through hydration, had mass ratios ranging from approximately 49.4 to 64.9 percent for alite and from 5.0 to 10.7 percent for C₂S. Additionally, the aluminate phase, whose hydration is controlled by the addition of calcium sulfate(s) to prevent flash set and enhance early-age mechanical strength, had mass ratios ranging from about 3.4 to 10.7 percent in the PLC samples. The C₄AF mass ratio ranged from 6.7 to 12.1 percent.

Based on phase identification through XRD data analysis, calcite was found to be the only polymorph of CaCO_3 present in the PLC samples. In addition, other cementitious phases detected in the PLC samples included dolomite ($\text{CaMg}(\text{CO}_3)_2$), gypsum ($\text{CaSO}_4 \cdot 2\text{H}_2\text{O}$), bassanite ($\text{CaSO}_4 \cdot 0.5\text{H}_2\text{O}$), and periclase (crystalline MgO), with average mass ratios of 2.1, 3.6, 2.0, and 1.0 percent, respectively. Notably, portlandite ($\text{Ca}(\text{OH})_2$) was also detected in all PLC samples, indicating that the PLCs were slightly prehydrated during handling from the cement plant to the testing time. The $\text{Ca}(\text{OH})_2$ content ranged from 0.2 to 1.1 percent, with an average mass ratio of 0.5 percent.

Figure 9. Graph. Mass ratio distribution of cementitious phases for PLC samples. A normal distribution was shown for comparison purposes. (♦ shows the average value for the data.)



Source: FHWA.

5.3 CaCO₃

CaCO₃ content indicated how much limestone was added to the cement to create the Type IL. However, the measurement is not direct because the limestone contains impurities. ASTM C595⁽²⁾ and AASHTO M 240⁽³⁾ specify minimum total carbonate and CaCO₃ contents of 70 and 40 percent, respectively, in the limestone used for producing blended cement.

CaCO₃ content in PLC samples was determined using a thermogravimetric analyzer (TGA). Figure 10 presents the variation in the CaCO₃ content of the tested PLCs. According to ASTM C595⁽²⁾ and AASHTO M 240⁽³⁾, the limestone used in PLC must have a minimum of 40 percent by weight CaCO₃ indicating that for a PLC with 5–15 percent by weight limestone, the quantity of CaCO₃ can range from 2.0 percent by weight (for limestone with 40 percent CaCO₃) to 15.0 percent by weight (for limestone with 100 percent CaCO₃). The data for the PLCs in this study show an average of

10.0 percent by weight CaCO₃, indicating an average limestone content between 10.0 percent by weight (for limestone with 100 percent CaCO₃) and 25.0 percent by weight (for limestone with 40 percent CaCO₃) for the tested PLCs. Half of the PLC samples have a CaCO₃ content between 8.4 and 10.3 percent by weight.

Limestone used for producing PLC typically comes from calcitic or dolomitic limestone rocks, although other sources, such as siliceous limestone, may also be used. Calcitic limestone primarily consists of calcite, with small amounts of dolomite, quartz, and other minor phases. Dolomitic limestone is similar to calcitic limestone but contains a significant amount of dolomite (CaMg(CO₃)₂), which contains both calcium and magnesium carbonates. Siliceous limestone, in turn, resembles dolomitic limestone but has lower dolomite content, along with higher levels of quartz and amorphous phases.⁽³²⁾ Based on the QXRD results

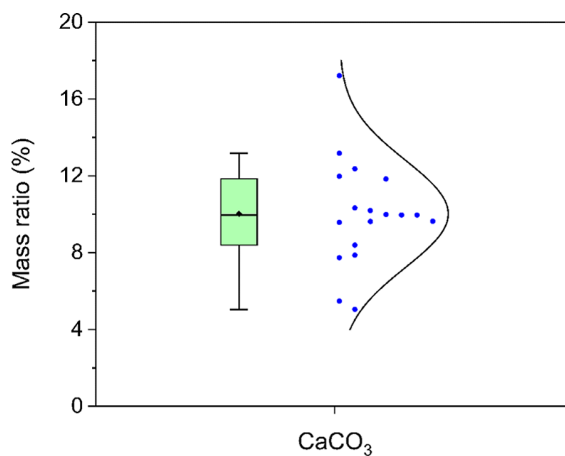
in figure 9, quartz is negligible in most of the PLCs (0.0–0.3 percent), while dolomite content ranges from 0.6 to 4.5 percent, suggesting that the limestone rock used to produce the studied PLCs was neither calcitic nor siliceous. The most likely type of limestone is dolomitic limestone. Given the negligible amorphous content in the PLCs, it can be inferred that the amorphous phase content in the limestone rock used was also negligible. Consequently, the limestone content in the PLCs can be estimated as the sum of calcite and dolomite contents. Based on the assumption that there are only two phases in dolomitic limestone in PLC samples, the limestone mass ratio in the studied PLCs ranges approximately 7–18 percent. Furthermore, based on this estimation, the limestone in the studied PLCs contained at least 70 percent CaCO_3 in the form of calcite. Note that according to a recent survey on 44 commercially available PLCs in the United States in 2022⁽⁵⁾, the mean limestone content was 10.5 ± 1.4 percent.

Because the density of limestone is lower than that of portland cement clinker, incorporating larger quantities of limestone reduces the density of PLC. Figure 11 illustrates a linear relationship between density and the quantity of CaCO_3 (from TGA); however, this correlation is not strong because the phase composition of limestone and clinker also influences the density of PLC.

LOI testing burns off the water and carbon, in the form of carbon dioxide (CO_2), within a cement. According to ASTM C114⁽²⁸⁾, LOI represents the total moisture and CO_2 content in the cement. Considering that the moisture uptake of freshly produced and delivered cement is limited (as validated via TGA measurements in this work), most of the LOI originates from CO_2 release, which indicates the presence of CaCO_3 in the cement. Therefore, CaCO_3 content can be related to LOI content. Figure 12 shows the linear relationship between CaCO_3 and LOI in the tested PLCs. This linear regression model can be used to estimate the quantity of CaCO_3 by measuring the LOI of PLC. The strong correlation shown in figure 12 suggests that most of the weight loss in PLCs is due to the decomposition of CaCO_3 , attributed to the high limestone content and its high purity.

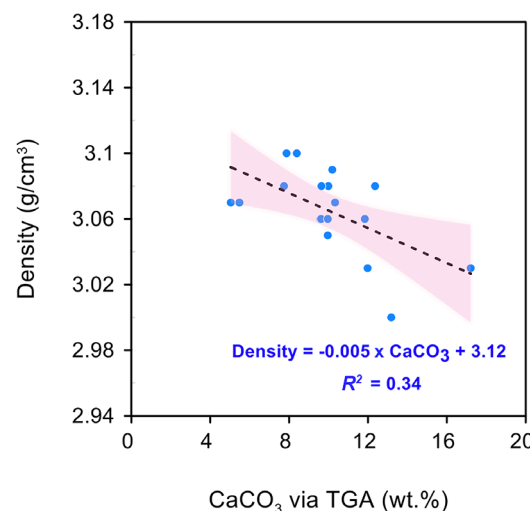
Despite the inherent calculation errors in measuring CaCO_3 through TGA and QXRD, the results indicate a linear relationship between the CaCO_3 content obtained from TGA and QXRD (figure 13). Such a strong correlation implies that TGA and QXRD can be used interchangeably to measure the CaCO_3 content in PLCs. However, due to simplicity and cost effectiveness, LOI measurement can be an appropriate method for comparing CaCO_3 content in PLCs.

Figure 10. Graph. Distribution and range of CaCO_3 content for PLC samples. A normal distribution was shown for comparison purposes. (♦ shows the average value for the data.)



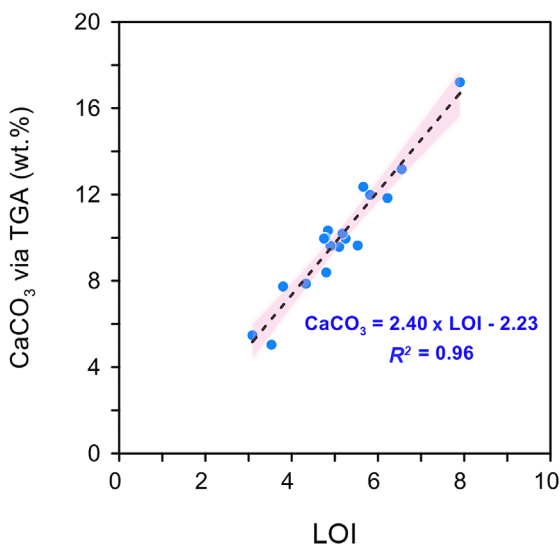
Source: FHWA.

Figure 11. Graph. Relationship between density of PLC and CaCO_3 obtained via TGA measurements. The highlighted area shows 95-percent confidence bands, and the dashed line is the trendline.



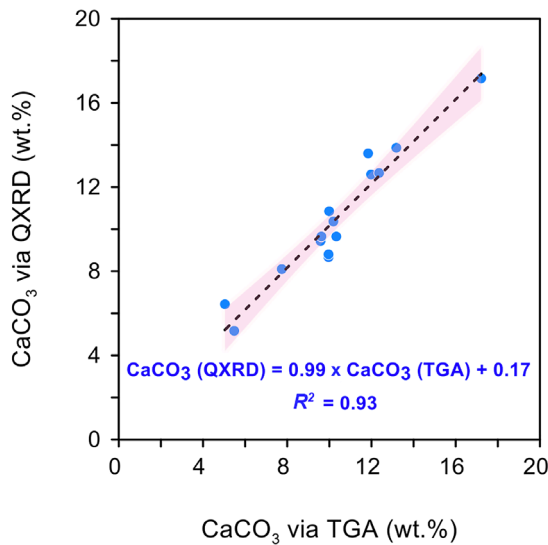
Source: FHWA.
wt. % = weight percent.

Figure 12. Graph. Relationship between CaCO_3 obtained via TGA measurements and LOI measured in accordance with ASTM C114⁽²⁸⁾ test method. The highlighted area shows 95-percent confidence bands and the dashed line is the trendline.



Source: FHWA.

Figure 13. Graph. Relationship between CaCO_3 obtained via QXRD analysis and TGA measurements. The highlighted area shows 95-percent confidence bands and the dashed line is the trendline.



Source: FHWA.

6. REACTIVITY

Chemical reactivity of PLC samples was assessed through measurements of heat release and setting times. To measure the reactivity of PLC samples, cement paste mixtures were prepared at two w/c (0.40 and 0.50) to cover a range of w/c practically used in the field for concrete mixtures.

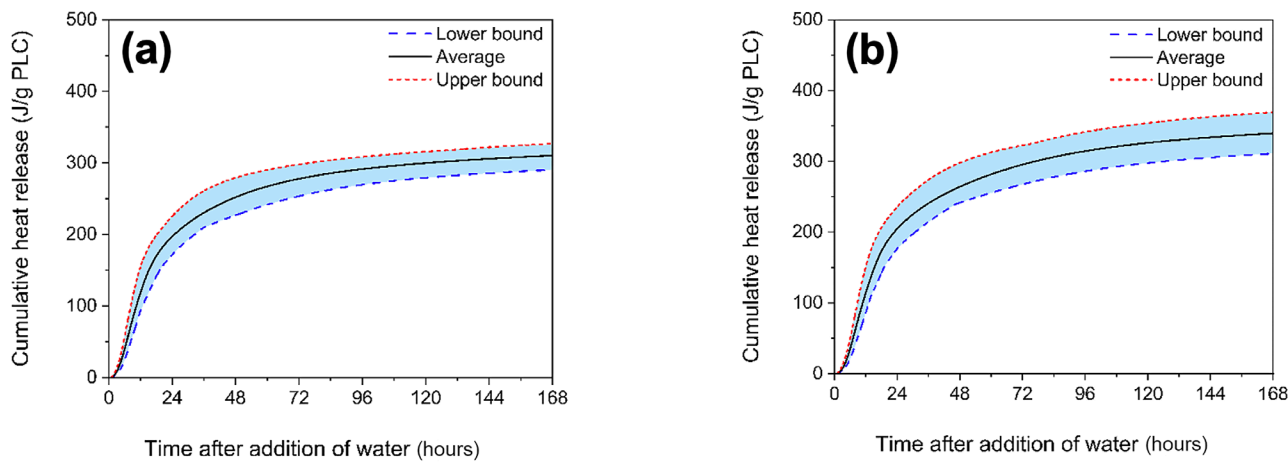
6.1 Isothermal Calorimetry

Isothermal calorimetry was conducted according to ASTM C1702 except that the PLC pastes were mixed outside of glass ampoules.⁽³³⁾ Cumulative heat release at a specific time is a measure of cement reactivity at that curing age. Cumulative heat release was measured through 7 d of curing. Figure 14 shows cumulative heat release for PLC paste mixtures at w/c of 0.40 and 0.50. As shown in figure 14, the 0.5 w/c led to higher cumulative heat release, particularly after the first day of reaction, suggesting that the cements generally did not achieve their highest practical degree of hydration at a w/c of 0.40.

Using cumulative heat data from figure 14, figure 15 presents the heat of hydration after 1 d, 3 d, and 7 d of reaction (from the time water was added to PLC) for both w/c of 0.40 and 0.50. According to figure 15, for PLC pastes with a w/c of 0.40, the heat of hydration after 1 d of reaction ranges from 172 to 226 J/g of PLC. Similarly, the heat of hydration for pastes with w/c of 0.50 ranges from 177 to 236 J/g of PLC. This similarity may be due to water and space availability for hydration within the first day of reaction. However, after 3 d, the cumulative heat of hydration ranges from 254 to 298 J/g of PLC for PLC pastes with a w/c of 0.40 and from 268 to 323 J/g of PLC for those with a w/c of 0.50. After 7 d of hydration, the heat of hydration ranges from 290 to 327 J/g of PLC for pastes with a w/c of 0.40 and from 311 to 369 J/g of PLC for a w/c of 0.50. This trend indicates that the variability in heat of hydration between PLC systems with varying w/c increases with age.

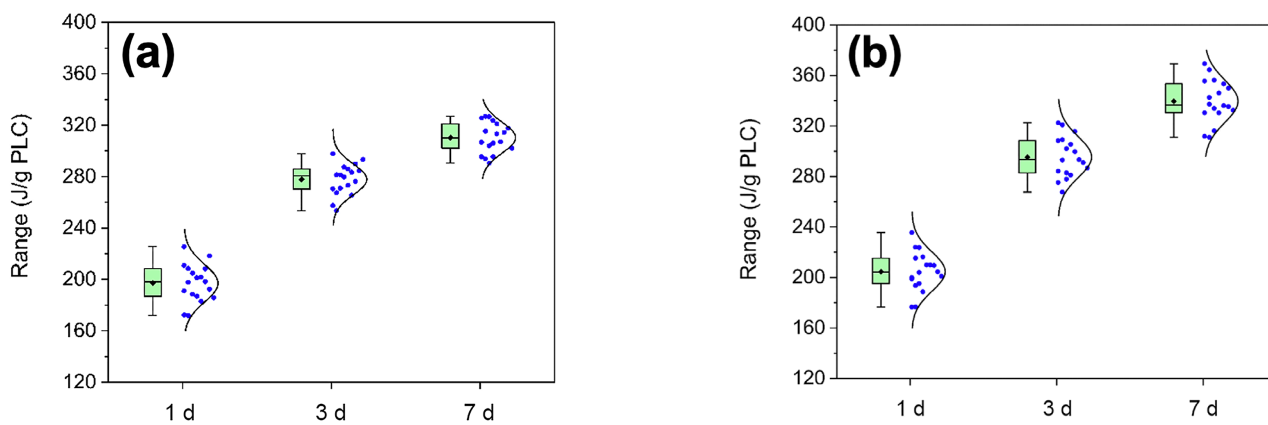
Ultimate heat of hydration (H_u) refers to the maximum cumulative heat released from a cementitious system due to the reaction of cementitious materials. The H_u represents the total heat released when the reactions (e.g., hydration in neat cement paste) cease. In other words, H_u refers to the total cumulative heat released when the cementitious system achieves its highest degree of hydration, which typically occurs when the available water for the reaction has been depleted through consumption or evaporation. For cement-based materials with sufficient water for reactions, it generally takes several years to reach the ultimate degree of hydration. For perspective, figure 16 schematically shows the H_u in comparison to the cumulative heat released up to 192 h (8 d) after the addition of water for a PLC paste.

Figure 14. Graph. Cumulative heat released during reactions of PLC paste mixtures at a w/c of (a) 0.40 and (b) 0.50. Dotted lines show maximum, dashed lines show minimum, and solid lines show average cumulative heat for all PLC paste mixtures tested in this study.



Source: FHWA.

Figure 15. Graph. Heat of hydration for PLCs after 1, 3, and 7 d of reaction for w/c of (a) 0.40 and (b) 0.50. A normal distribution was shown for comparison purposes. (♦ shows the average value for the data.)



Source: FHWA.

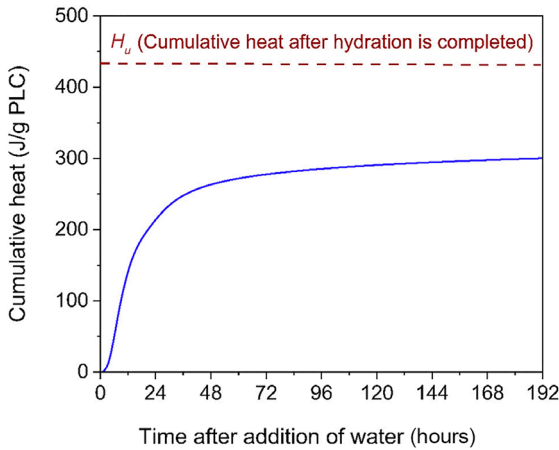
To obtain H_u of PLCs at each w/c, an exponential model⁽³⁴⁾ (equation 1) was fitted to the cumulative heat release data (figure 14) and the results are shown in figure 17.

$$H_u = \frac{H_t}{e^{-(\frac{\tau}{t})^\beta}} \quad (\text{Equation 1})$$

where H_t is the cumulative heat release (J/g PLC) at time t (h) after mixing, H_u is the ultimate heat of hydration of PLC, and τ and β are fitting parameters.

According to figure 17, the H_u of PLC increases with a higher w/c (0.50), likely due to the greater availability of water and space for hydration to progress. Furthermore, as shown in figure 17, greater variability in H_u was observed for PLC paste with a higher w/c (0.50). In contrast, the lower variability of H_u data at a lower w/c (0.40) suggests insufficient water for further PLC hydration, leading to more similar H_u values among the studied PLCs and diminishing influence of the physical and chemical characteristics of PLC on its maximum degree of hydration. This finding underscores that, in addition to the physical and chemical properties of PLC, the w/c plays a pivotal role in determining the degree of hydration in PLC systems.

Figure 16. Graph. Schematic representation of the H_u compared to the cumulative heat released for a PLC paste up to 200 h (w/c = 0.50).



Source: FHWA.

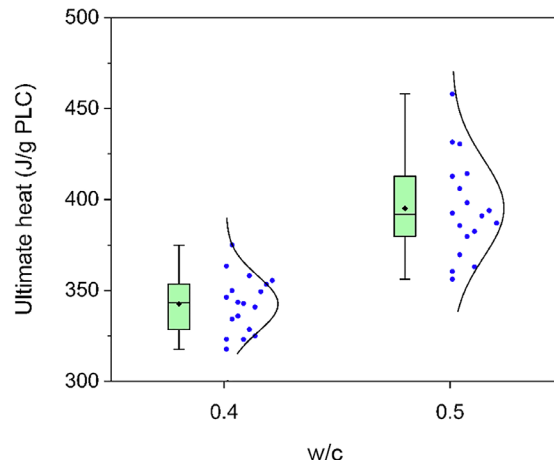
6.2 Factors Affecting PLC Hydration

Cement reactivity depends on its physical and chemical properties. However, the effect of these factors varies based on the type of cement, such as OPC and PLC.

To assess the impact of the physical and chemical characteristics of PLC on its early-age reactivity (up to 7 d), a Spearman's correlation analysis⁽³⁵⁾ was conducted at a significance level of 0.05. Because the characteristics and reactivity data of PLCs do not follow a normal distribution, Spearman's statistical test, a nonparametric analysis that does not require normality, was employed.

Figure 18 presents the results of the correlation analysis between the physical characteristics of PLC and its reactivity at various curing ages up to 7 d. As seen in figure 18, all particle size indices have a statistically significant effect on the 1-d cumulative heat release; however, their effect on the 3-d and 7-d cumulative heat release is not statistically significant, indicating a statistically significant effect of particle size distribution on the initial (first 24 h) reactivity of PLC. The primary reaction process of portland cement within the first 24 h is nucleation and growth, with the dissolution rate of cement particles playing a key role in reactivity during this period. Since finer cement particles show more rapid reactivity (either from finer clinker particles that

Figure 17. Graph. H_u for PLC paste with: (a) w/c = 0.40 and (b) w/c = 0.50.



Source: FHWA.

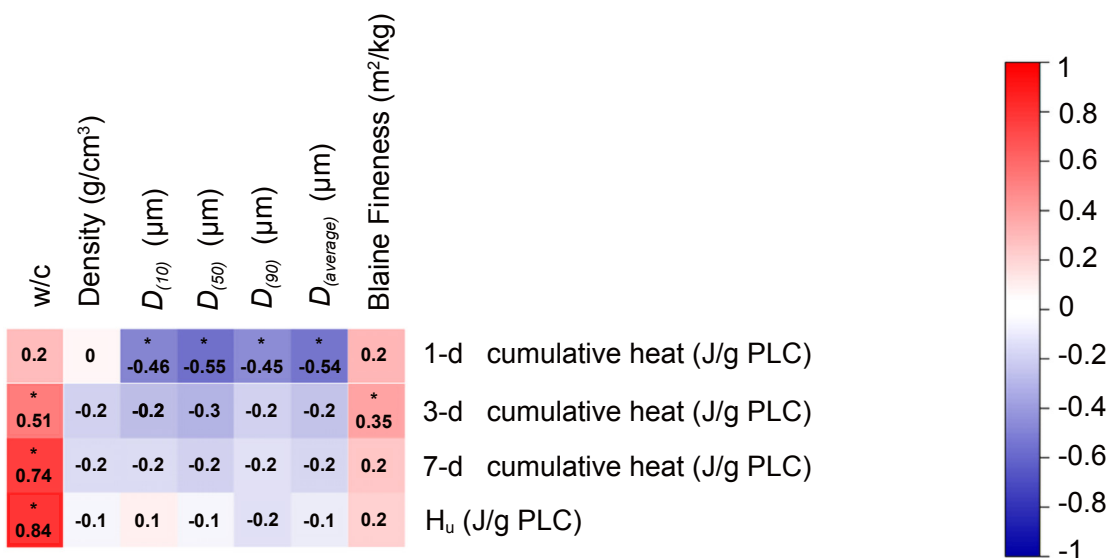
dissolve more quickly in water and/or finer limestone particles that accelerate clinker hydration) finer PLC is expected to exhibit increased reactivity during the first 24 h of hydration, as indicated by the negative correlation coefficients in figure 18. Moreover, Blaine fineness exhibits a negligible or nonsignificant influence on the early-age reactivity of PLC, as indicated by its low correlation coefficient. This lack of correlation suggests that the Blaine fineness test may not be a reliable indicator of PLC reactivity. Such a negligible effect of Blaine fineness on PLC's early-age reactivity could be attributed to the finer nature of PLC compared to OPC, for which the Blaine test was originally developed and validated. In addition, w/c has a greater impact on PLC reactivity as reaction time increases, highlighting the importance of water availability for the continued hydration of PLC at later ages.

According to figure 18, producing finer PLC can enhance very early-age reactivity (first 24 h), which has implications for developing high early-strength

concretes. Furthermore, the w/c should be adjusted for PLC concretes and proper curing methods should be implemented to ensure sufficient water availability in the system, which is crucial for maximizing PLC's early-age reactivity and essential for opening roads to traffic.

The oxide composition of cement provides valuable insight into the reactivity of portland cement.^(20,27) However, it remains unclear which oxide(s) have the greatest influence on the reactivity of PLC. Figure 19 shows the results of the correlation analysis between various combinations of the oxide composition of PLC and its reactivity at different curing ages. As depicted in figure 19, both Al_2O_3 and SO_3 have a statistically significant effect on the 1-d reactivity of PLC, indicating that the aluminate and sulfate contents have a substantial impact on the early age reactivity of PLC. Specifically, SO_3 content directly increases the 1-d total heat release, while the quantity of Al_2O_3 has an opposite effect, reducing the 1-d total heat release of PLC.

Figure 18. Image. Correlation matrix of hydration indices³ and physical characteristics for the studied PLCs. (The numbers in the boxes show Spearman's correlation coefficient and the asterisk indicates that the correlation is statistically significant at a 0.05 significance level.)



Source: FHWA.

³Hydration indices are 1 d, 3 d, 7 d, and the H_u .

The alkali contents (Na_2O and K_2O and therefore the combined alkali content shown as $\text{Na}_2\text{O}_{\text{eq}}$) show a statistically significant effect on the early-age reactivity of PLC (up to 7 d). While K_2O has a greater impact on the 1-d total heat release of PLC, Na_2O is more influential on the 3-d and 7-d reactivity. In general, higher alkali contents increase the pH of the pore solution, resulting in accelerated dissolution and hydration of cementitious phases. Additionally, MgO content has an inverse effect on the 1-d reactivity of PLC; however, MgO 's low correlation coefficient with the 1-d heat of hydration suggests that this effect is not significant.

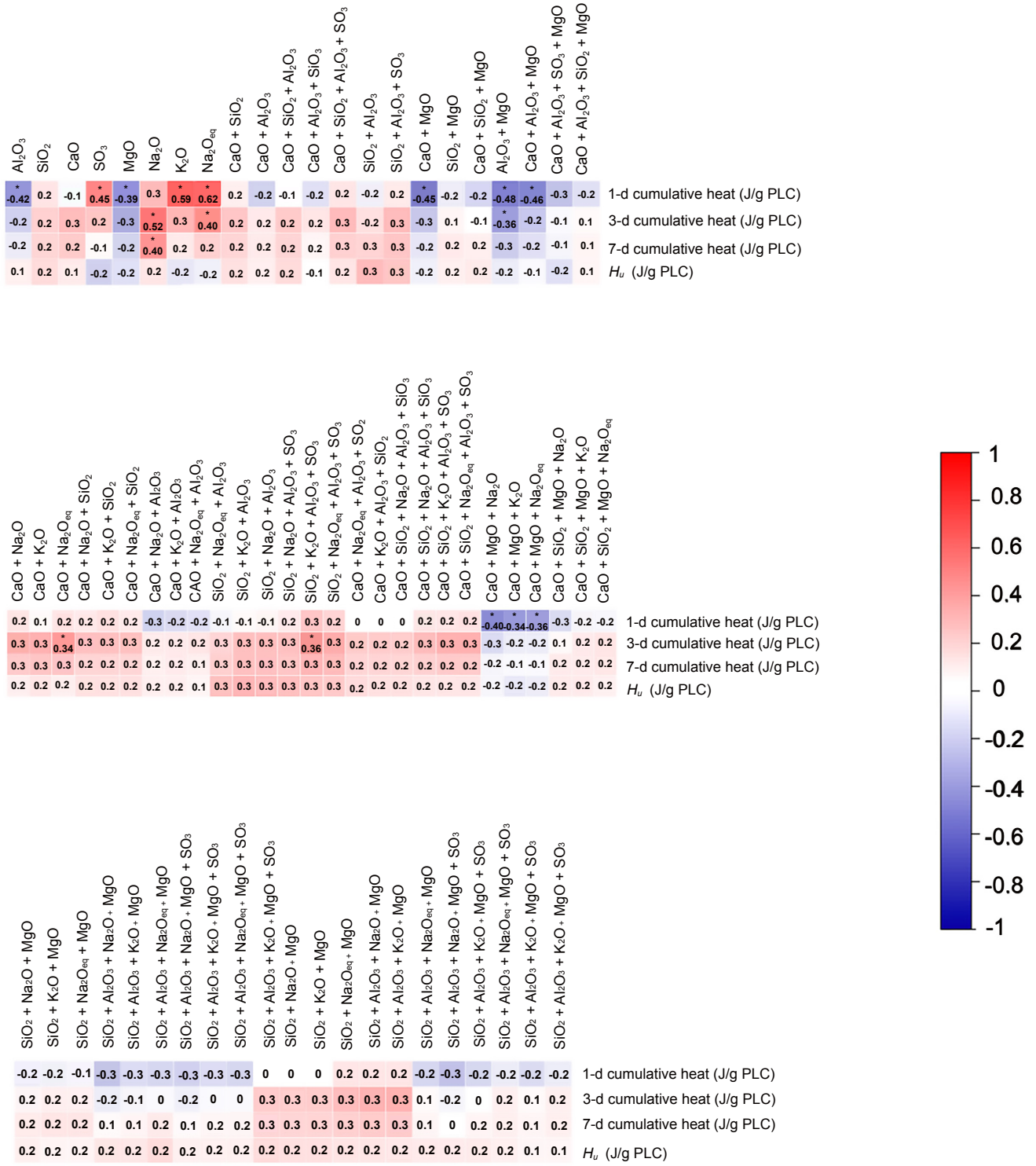
In addition to examining the influence of individual oxides, combinations of oxides were analyzed to evaluate their collective effect on the reactivity of PLC. The combination of Al_2O_3 and MgO exhibited an inverse effect on the 1-d cumulative heat, similarly to their individual effects. This inverse effect extended to the 3-d cumulative heat when Al_2O_3 and MgO were combined. Furthermore, this combination also demonstrated an inverse effect on 1-d cumulative heat when combined with CaO . The combination of CaO and MgO showed an inverse effect on the 1-d cumulative heat. This effect overshadowed the direct influence of alkalis on the 1-d cumulative heat, resulting in an overall inverse effect when CaO , MgO , and alkali oxides were combined.

As shown in figure 19, limiting MgO content in PLC may benefit its very early-age (first 24 h) reactivity, which has implications for higher early strength. Additionally, when PLC has high alumina content, SO_3 level should be adjusted to enhance reactivity during the first day of hydration, highlighting the importance of sulfate optimization in PLC systems during the production stage. Although alkali content positively influences the reactivity of PLC, due to concerns about alkali-silica reaction, it is advisable to limit their levels.

Figure 20 illustrates the results of the correlation analysis between hydration indices and the phase composition of PLC. As shown, unlike the w/c, there is no statistically significant correlation between H_u and the cementitious phase composition of PLC. This lack of correlation can be attributed to the limited variation in the mass ratio of cementitious phases in the tested PLCs, because the limestone⁴ replacement ratio is also relatively narrow (most PLCs contained 10–15 percent limestone according to their mill test reports). This narrow replacement ratio suggests that cement plants aim to maximize limestone replacement to reduce costs and improve resource efficiency, resulting in minimal changes in the mass ratio of the remaining cementitious phases.

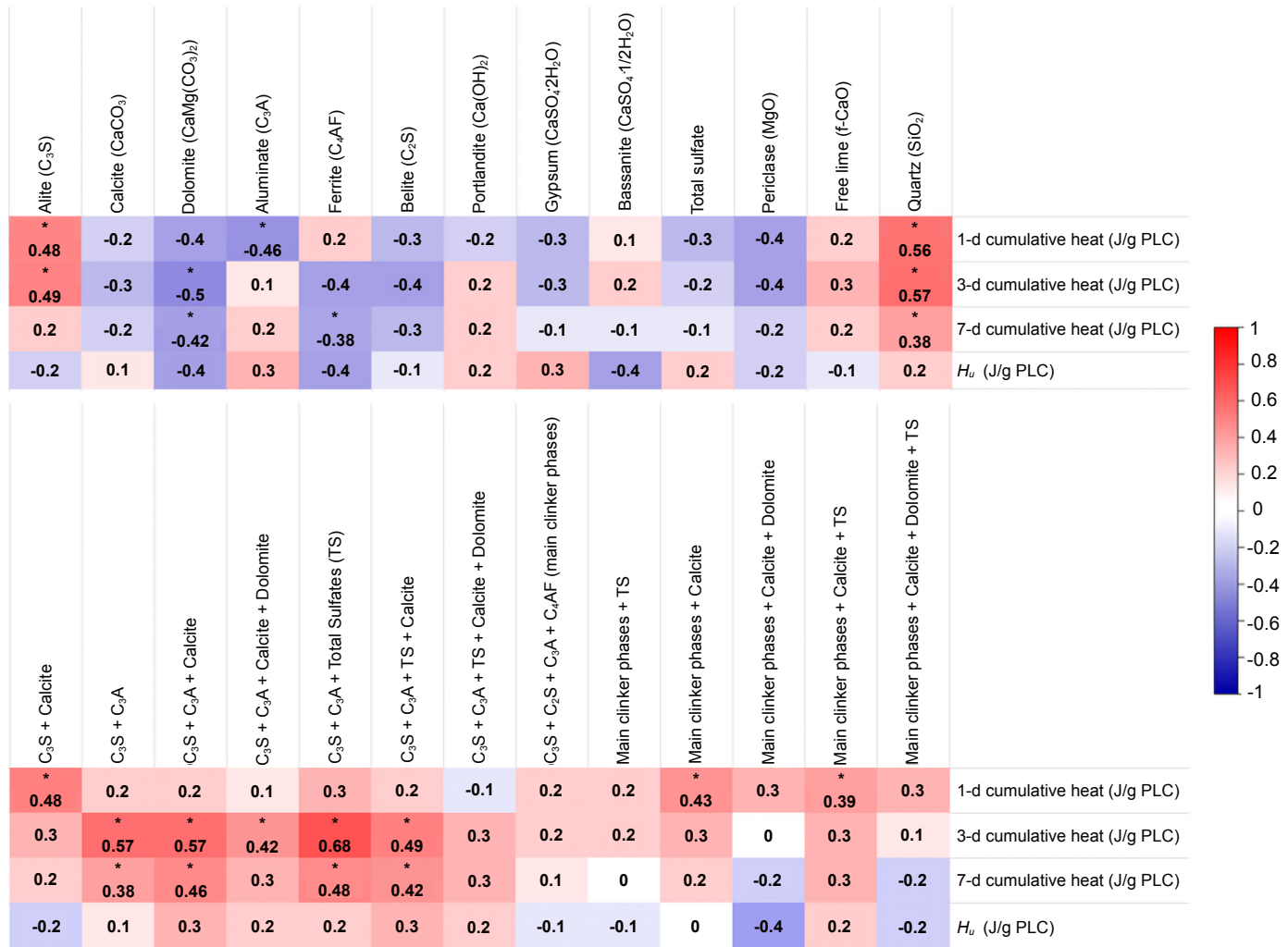
⁴This study assumed that the limestone consists solely of calcite and dolomite, without any impurities. This assumption holds true for dolomitic limestone, a primary feedstock used in cement plants for producing PLC.

Figure 19. Correlation matrix of hydration indices and oxide composition for the studied PLCs. (The numbers in the boxes show Spearman's correlation coefficient and the asterisk indicates that the correlation is statistically significant at a 0.05 significance level.)

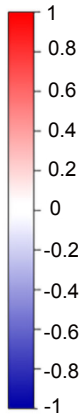


Source: FHWA.

Figure 20. Image. Correlation matrix of hydration indices and cementitious phase composition for the studied PLCs. (The numbers in the boxes show Spearman's correlation coefficient and the asterisk indicates that the correlation is statistically significant at a 0.05 significance level. Total sulfates (TS) = gypsum + bassanite. Main clinker phases = $C_3S + C_2S + C_3A + C_4AF$.)



Source: FHWA.



Alite demonstrated a statistically significant correlation with 1-d and 3-d cumulative heat, highlighting its critical role in early hydration and, consequently, in the strength development of PLCs. Additionally, the combined effect of alite and calcite showed a statistically significant correlation with 1-d cumulative heat, underscoring calcite's role in accelerating hydration during the first 24 h.

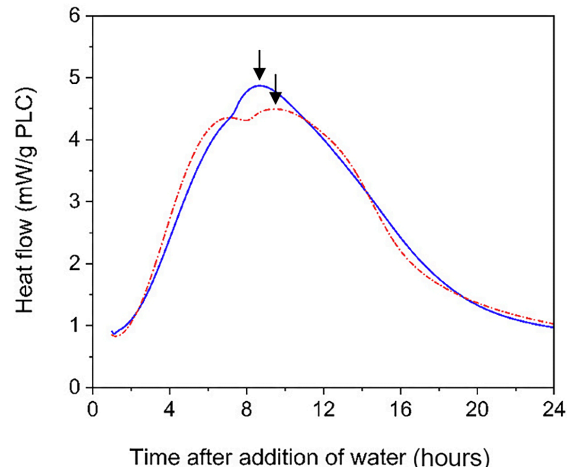
PLC systems are more prone to undersulfation than OPC systems, leading to higher variability in performance of PLCs during very early ages (first 24 h). In PLC systems, the incorporation of fine limestone particles accelerates sulfate removal from the pore solution due to their enhancing effect on alite hydration. Enhancement in alite reactivity leads to the faster formation of C-S-H, which adsorbs sulfate ions from the pore solution, further accelerating their depletion.⁽³⁶⁾ Since calcium sulfates are added to cement to ensure the renewed reaction of aluminate occurs after final set but in the first 24 h to contribute to early-age mechanical strength, more precise sulfate adjustments are needed in PLCs to optimize the involvement of cementitious phases in the hydration process.

According to figure 19, aluminate exhibited an inverse effect on the 1-d cumulative heat, indicating that the renewed reaction of aluminate—regulated by sulfate addition—was not sufficiently controlled in the studied PLCs. A similar inverse effect of alumina and a direct effect of SO_3 on the 1-d cumulative heat of PLCs were observed. Improper adjustment of the sulfate level may negatively impact the early hydration of PLC, primarily due to reduced alite reactivity. Aluminate reactions can interfere with alite hydration, resulting in a reduced hydration degree during the first few hours of hydration (less than 24 h).⁽³⁷⁾ For context, figure 21 illustrates how the renewed hydration of aluminate interferes with the alite reaction peak (solid-line curve) and higher renewed aluminate peak than the alite peak highlighting improper sulfate addition in PLC systems (both curves).

According to figure 20, alite and aluminate demonstrated a statistically significant correlation with 3-d and 7-d cumulative heat. This result is expected because alite directly influences 1-d and 3-d hydration, while aluminate shows an inverse effect on 1-d hydration, possibly due to sulfate imbalance in the PLC systems. Together, these two phases exhibit a synergistic effect on hydration beyond the first 24 h, attributed to the extended renewed hydration of aluminate beyond the first day (figure 22). Figure 22 shows that the renewed hydration of aluminate (shown by arrows) was extended to the second day of PLC hydration, highlighting the importance of adjusting sulfate content to ensure the contribution of renewed aluminate hydration to the first day of PLC reactivity, which leads to higher mechanical strength development in PLC paste and has

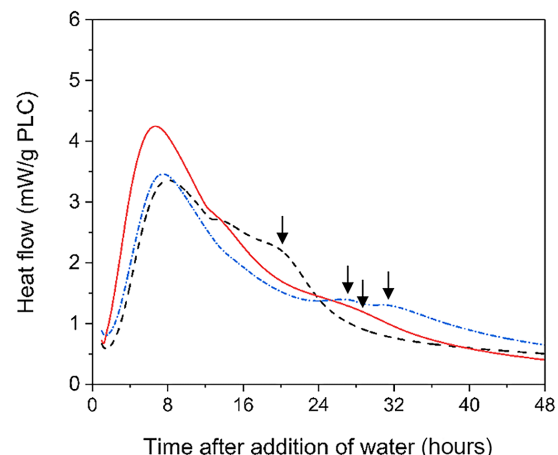
implications for high early-strength concrete. Furthermore, the correlation coefficient between the combined mass of alite and aluminate and 3-d and 7-d hydration, shown as $\text{C}_3\text{S}+\text{C}_3\text{A}$, compared with 3- and 7-d cumulative heat in figure 20 increased with the addition of sulfates (gypsum and bassanite), shown as $\text{C}_3\text{S}+\text{C}_3\text{A}+\text{TS}$. This statistically significant correlation underscores the importance of maintaining sulfate balance in PLC systems to enhance reactivity and, consequently, early strength development.

Figure 21. Graph. Elevated renewed aluminate reaction peak indicating improper sulfate additions in two different PLC systems. (Arrows denote the renewed aluminate peak.)



Source: FHWA.

Figure 22. Graph. Extended renewed aluminate reaction in several PLC systems. (Arrows denote the renewed aluminate peak.)



Source: FHWA.

Based on figure 20, the addition of calcite (high-purity limestone) increased the correlation coefficient between the combined mass of alite and aluminate and 7-d hydration compared to alite and aluminate alone. This correlation highlights the beneficial effect of calcite on early-age (7 d) hydration of PLC.

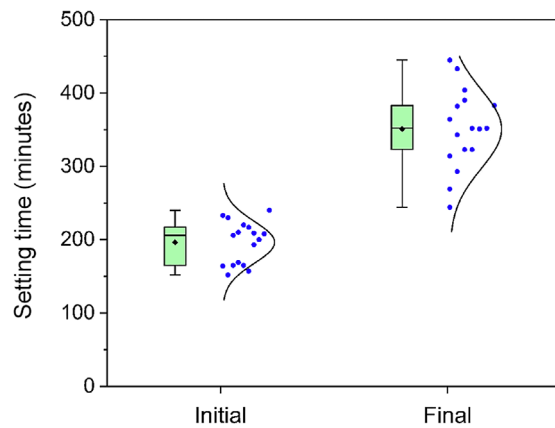
Dolomite exhibited an inverse effect on 3-d and 7-d cumulative heats, indicating that limestone impurities are unfavorable to the reactivity of PLCs. Additionally, quartz content showed a statistically significant effect on the hydration of PLCs up to 7 d. However, its content, ranging from 0.0 to 1.1 percent (with an average of 0.3 percent), is relatively low. Considering its limited solubility in the cementitious matrix, this correlation may not hold practical significance.

As indicated by the correlation analysis in figure 20, the use of limestone with higher purity results in higher reactivity of PLCs. Furthermore, sulfate adjustment plays a crucial role in the early contribution of renewed aluminate hydration, ensuring higher reactivity of PLCs during the first 24 h, which is essential for high early-strength concrete materials.

6.3 Setting Time

Setting time is an indicator of physical changes in cement paste resulting from the chemical reactivity of cement particles. The initial setting time represents the age (from the addition of water) when the cement paste begins to solidify or lose its plasticity, while the final setting time is the age (from the addition of water) at which the paste loses plasticity and strength begins to develop at a significant rate. Setting times correlate only to the very early reactivity (in the first few hours of hydration) of cementitious materials and, therefore, do not provide a comprehensive understanding of the hydration kinetics of cement particles. However, setting times are used in the field to indicate length of workable time with a concrete mixture and when to finish, cure, and saw cut.

Figure 23. Graph. Distribution and range of initial and final setting times for PLC pastes. A normal distribution was shown for comparison purposes. (♦ shows the average value for the data.)



Source: FHWA.

The setting times of PLC pastes were measured using a Vicat apparatus according to ASTM C191.⁽³⁸⁾ Measurements were conducted on PLC pastes with a w/c of 0.40 because some PLC paste samples with a w/c of 0.50 exhibited a thin layer of water due to bleeding.

Figure 23 presents the results of the setting time measurements. According to figure 23, the initial setting time data are less variable than the final setting time data for the PLC samples tested. The initial setting times ranged from approximately 150 to 230 min, while the final setting times ranged from 240 to 450 min.

Furthermore, correlation analysis was conducted using the method outlined in section 6.2 of this document. The results indicated that none of the physical or chemical characteristics of PLCs had a statistically significant impact on the initial or final setting times of PLC paste.

7. BATCH VARIATION

Four PLC samples were collected over a 15-mo period from one cement plant, enabling evaluation of the impact of batch variations on the physical and chemical properties of PLC and their reactivity. All samples were designated as Type IL(10) based on the mill test reports. Note that PLC type is designated by its limestone content, Type IL(X), where X represents the limestone weight percentage in PLC. ASTM C595⁽²⁾ and AASHTO M 240⁽³⁾ allow a tolerance of up to 2.5 percent by weight in limestone content.

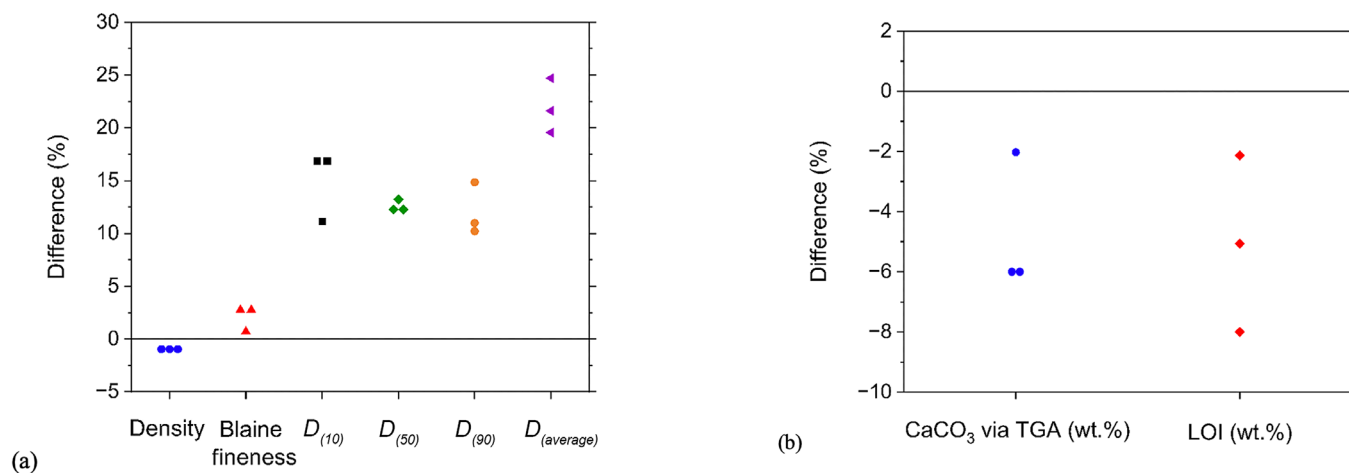
For comparison, all data were normalized to the most recently acquired PLC batch (control batch), which serves as a more accurate representation of the current production technology in the cement industry, given the likelihood of advancements since PLC production at scale became widespread.

Figure 24 illustrates the variation in the physical characteristics of PLCs. The density and Blaine fineness

exhibit minimal variation (up to 3 percent), whereas the particle size distribution indicators ($D_{(10)}$, $D_{(50)}$, and $D_{(90)}$) show greater variability (up to 18 percent), with the average particle size displaying the highest variation (up to 25 percent). As noted earlier and shown in figure 5, all PLCs, including these four samples from the same plant, exhibited three humps in their particle size distribution. This characteristic contributes to the higher variation in average particle size because it represents all particle size fractions and reflects the variations across these fractions. Based on figure 24b, both LOI and CaCO_3 content (via TGA) show narrow and very similar variation (up to 8 percent) indicating correlation among their data as discussed in section 5.3 of this document (figure 12).

Figure 25 and figure 26 show the weight variation in the chemical characteristics of Type IL(10) batches, specifically oxide composition and cementitious phase composition, respectively. As depicted in figure 25, alkali oxides (Na_2O and K_2O), MgO , and Cr_2O_3 exhibit the highest variation (up to 52 percent). The concentrations

Figure 24. Graph. Comparison of (a) physical characteristics and (b) CaCO_3 content and LOI of different Type IL(10) batches from one facility with the most recently acquired batch. The percentage difference is calculated relative to the control batch.



Source: FHWA.

of these oxides affect strength development and hydration reactions.⁽³⁹⁾ Alkalies can cause alkali-silica reaction, which is expansive and can cause concrete cracking.⁽⁴⁰⁾ MgO mainly affects volume stability of cementitious materials.⁽³⁹⁾ Meanwhile, Manganese(III) oxide (Mn_2O_3), phosphorus pentoxide (P_2O_5), zinc oxide (ZnO), and strontium oxide (SrO) display up to 15 percent variation. In contrast, Al_2O_3 , SiO_2 , CaO , SO_3 , Fe_2O_3 , and titanium dioxide (TiO_2)—comprising the majority of the oxide composition—show minimal variation (≤ 8 percent). These results indicate that, while the variation in impurity weights is significant, the major oxides, which constitute 90–92 percent by weight of the PLC composition, remain highly consistent across different batches.

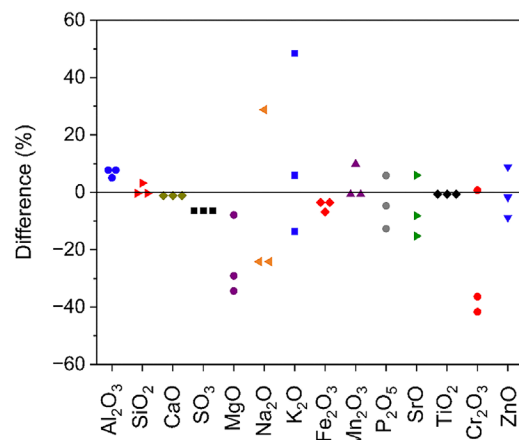
Figure 26 shows that the variation in calcium silicates (C_3S and C_2S), C_4AF , and calcite is minimal (≤ 25 percent), while aluminite (C_3A), dolomite, and free lime (CaO) exhibit variations of up to 54 percent compared to the control batch. Specifically, for alite, which is the primary cementitious phase responsible for the early-age reactivity of PLCs and subsequent strength development, the maximum variation is 10 percent.

Variations in calcium sulfate sources of gypsum and bassanite reach up to 200 and 100 percent compared to the control batch, respectively. The significant variation in calcium sulfate content may be attributed to fluctuations in aluminate content because sulfates play a key role in regulating aluminate reactivity.

The relatively high variation in dolomite content indicates notable inconsistencies in the purity of the limestone used for PLC production over time. However, ASTM C595⁽²⁾ and AASHTO M 240⁽³⁾ standards permit a 2.5 percent by weight variation in limestone content, meaning that Type IL(10) can contain 7.5–12.5 percent by weight limestone. The required purity of limestone per ASTM C595⁽²⁾ and AASHTO M 240⁽³⁾, in terms of carbonate content ($CaCO_3$ and dolomite), is 70 percent, which can contribute to the observed high variation in dolomite weight.

$Ca(OH)_2$ variation reached up to 68 percent, indicating that prehydration of PLC is highly influenced by handling procedures. Quartz has a consistent weight percentage of 0 percent across all PLC batches, resulting in minimal variation; however, its very small quantity leads to higher error in QXRD calculations, complicating the comparison process. Periclase exhibits the highest variation among all cementitious phases, with differences of up to 300 percent across various PLC batches. The hydration of periclase is

Figure 25. Graph. Comparison of the weight percentages of oxide compositions across four Type IL(10) batches relative to the control batch.



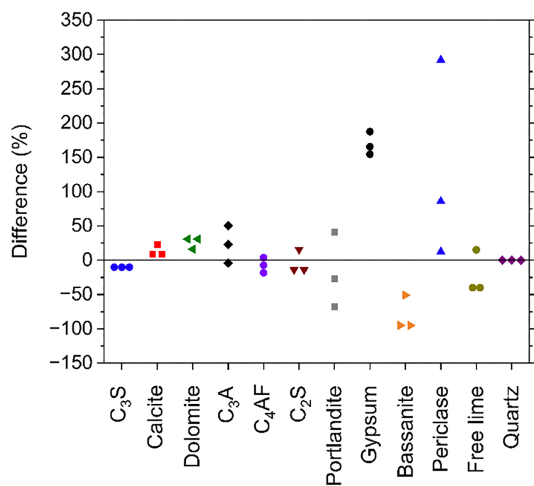
Source: FHWA.

expansive and can induce stresses in the hardened cement matrix that can cause concrete cracking and lead to further durability issues.⁽⁴¹⁾

Figure 27 presents the variations in initial and final setting times for PLCs from different batches compared to the control batch ($w/c = 0.40$). As shown in figure 27, the initial setting time exhibits less variability than the final setting time. This trend was also observed in figure 23, where greater variability was noted in the final setting time of PLCs.

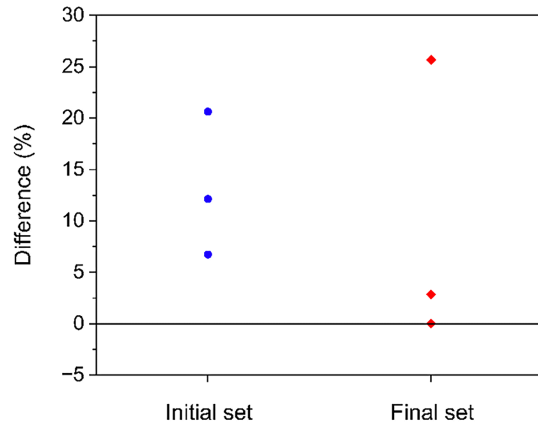
Figure 28 illustrates the variations in the cumulative heat of hydration for PLCs from different batches compared to the control batch at w/c of 0.40 and 0.50. This figure shows that the variation in cumulative heat of hydration during the early age (up to 7 d) is minimal (up to 5 percent) for both w/c when compared to the PLC paste made with the control batch. To further assess the impact of batch variation on PLC reactivity, a one-way ANOVA⁽⁴²⁾ test was conducted, revealing no significant differences in the heat of hydration among four PLC batches for either w/c . This consistency in Type IL(10) reactivity is attributed to minimal variations in the physical and chemical characteristics of PLCs, which are key factors influencing early-age reactivity, including average particle size (up to 25 percent variation), major oxides, including Al_2O_3 , SiO_2 , CaO , SO_3 , and Fe_2O_3 (up to 8 percent variation), and alite (up to 10 percent variation).

Figure 26. Graph. Comparison of the weight percentages of cementitious phase compositions across four Type IL(10) batches relative to the control batch.



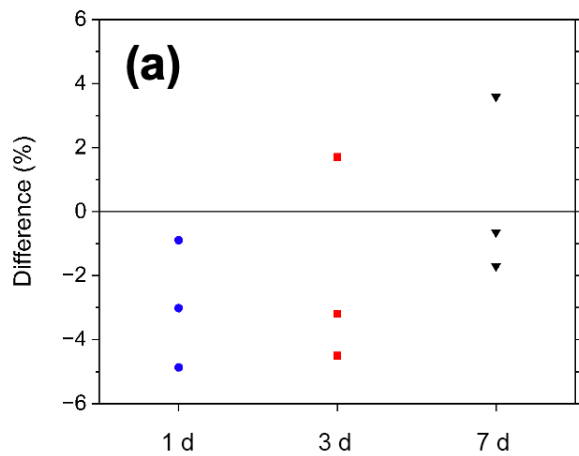
Source: FHWA.

Figure 27. Graph. Comparison of the initial and final setting times across four Type IL(10) batches relative to the control batch.

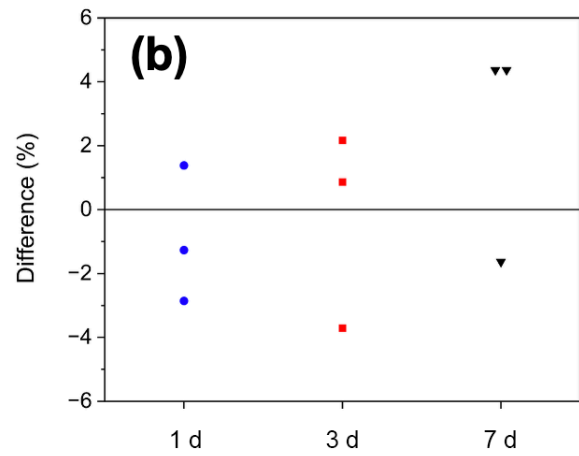


Source: FHWA.

Figure 28. Graph. Comparison of heat of hydration during early age (up to 7 d) across different Type IL(10) batches relative to the control batch: (a) w/c = 0.40 and (b) w/c = 0.50.



Source: FHWA.



8. VARIABILITY IN MILL TEST RESULTS

According to ASTM C595⁽²⁾ and AASHTO M 240⁽³⁾, several physical, chemical, and performance characteristics must be reported in PLC mill test results, including SO₃ content (ASTM C114)⁽²⁸⁾, LOI (ASTM C114)⁽²⁸⁾, equivalent alkali (Na₂O_{eq}) content (ASTM C114)⁽²⁸⁾, CaCO₃ in limestone (ASTM C114)⁽²⁸⁾, Blaine fineness⁽²²⁾, retained percentage on the No. 325 sieve (ASTM C430 or ASTM C1891)^(43, 44), density (ASTM C188)⁽²⁵⁾, mortar air content (ASTM C185)⁽⁴⁵⁾, initial setting time (ASTM C191)⁽³⁸⁾, mortar compressive strength (ASTM C109)⁽²¹⁾, and mortar bar expansion (ASTM C1038)⁽²⁹⁾ test results if the SO₃ mass ratio in PLC exceeds 3 percent. However, in the 2024 revisions of ASTM C595⁽²⁾ and AASHTO M 240⁽³⁾, autoclave expansion and contraction limits were removed compared to their 2021 versions. Additionally, measuring the heat of hydration at 3 and 7 d is no longer required, as moderate heat of hydration and low heat of hydration have been removed from the list of special PLC properties. Although not for all characteristics, there is a specification limit for most of PLC properties, as indicated by ASTM C595⁽²⁾ and AASHTO M 240.⁽³⁾

Figure 29 to figure 33 present measurement data from mill test reports provided by the manufacturers of the PLCs used in this study. Since the PLC samples were produced between 2022 and 2025, mill test reports were unavailable for some samples, and the reported data varied, as some manufacturers followed the 2021 version of ASTM C595⁽²⁾ and AASHTO M 240⁽³⁾ while others adhered to the 2024 version. Consequently, figure 29–figure 33 display only the characteristics reported by all manufacturers. Specification limits, if applicable, are indicated for each characteristic.

According to figure 29, among the chemical characteristics, Na₂O_{eq} content exhibited the highest variability, followed by the CaCO₃ content in the limestone used in PLCs. The variability in Na₂O_{eq} content is linked to variations in the characteristics of cement clinker, while the variation in CaCO₃ content reflects changes in the standard requirements, allowing

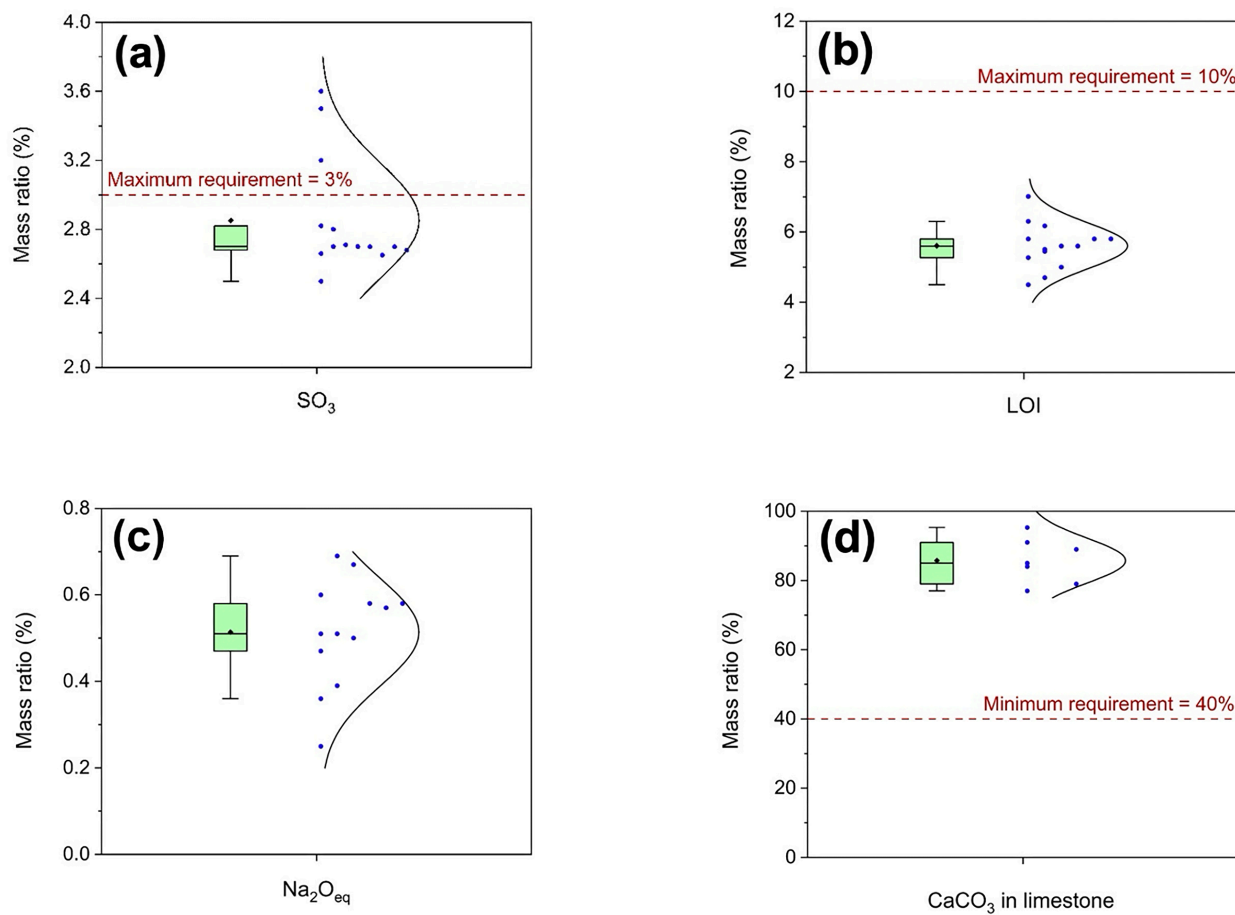
for a lower CaCO₃ content in limestone—from a minimum of 70 percent by weight CaCO₃ in limestone to a minimum of 40 percent for PLC production, as outlined in the 2021 and 2024 versions.

Furthermore, the LOI content ranges from 4.5 to 7.0 percent, well below the maximum allowable LOI of 10 percent. Additionally, most of the PLCs (almost 80 percent) had lower SO₃ content than the required 3 percent, thus eliminating the need for mortar bar expansion testing. However, PLCs exceeding the 3-percent SO₃ threshold exhibited lower expansion than the specification limit of 0.020 percent, as outlined by ASTM C595⁽²⁾ and AASHTO M 240.⁽³⁾

As shown in figure 30, the variability in density is the lowest, while PLCs exhibited higher variability in their fineness characteristics (Blaine fineness and retained content on the No. 325 sieve). The Blaine fineness ranged from approximately 400 to 550 m²/kg, while the retained quantity of PLCs on the No. 325 sieve (45 µm) varied from 0.0 to 5.1 percent. Additionally, 93 percent of PLCs had a density below 3.10 g/cm³.

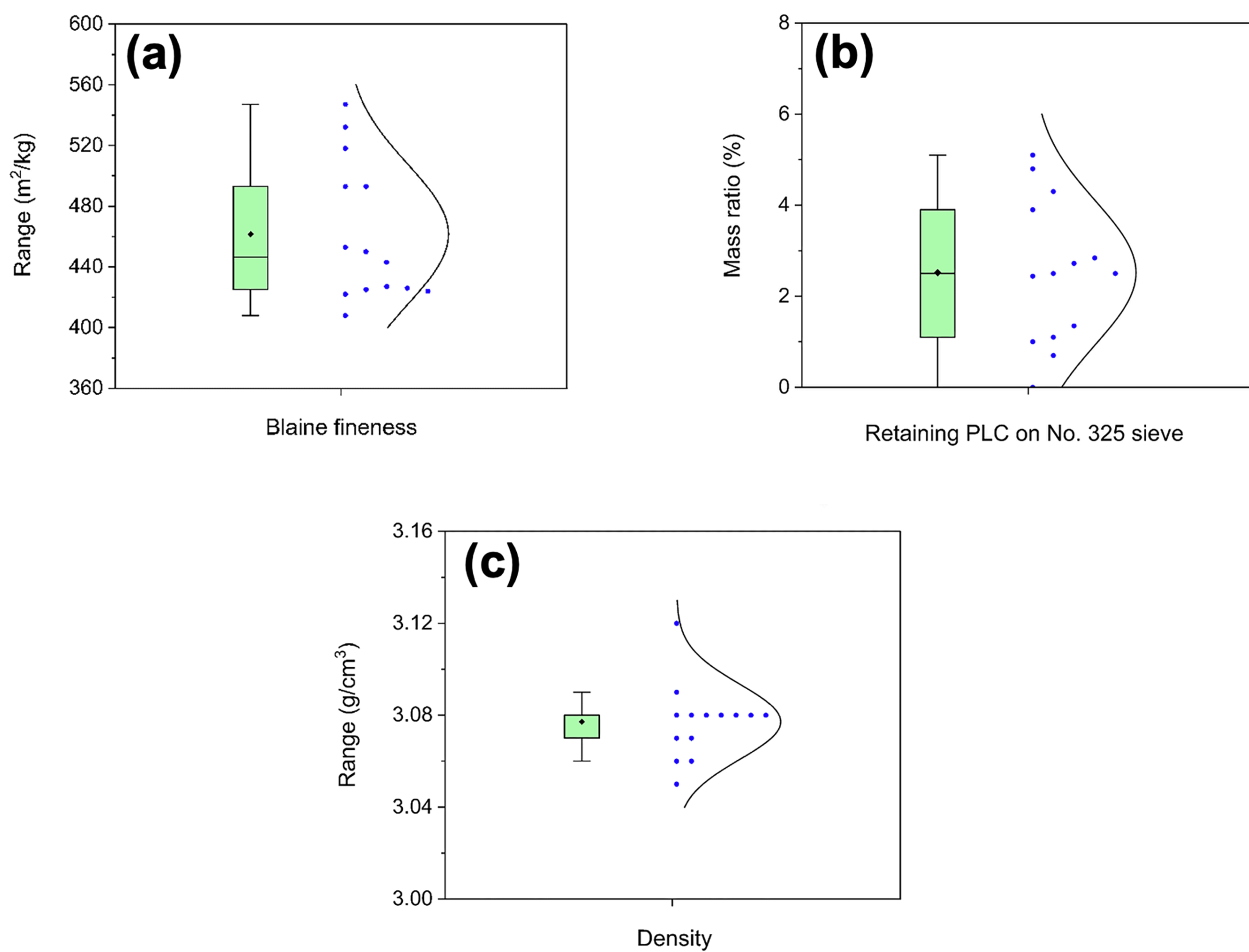
Initial setting time, air content in mortar, and compressive strength of mortar are key tests for evaluating the reactivity performance of PLC in cementitious materials. According to figure 31, despite variations in the chemical and physical characteristics of PLCs, the initial setting time showed minimal variation, with almost 93 percent having an initial setting time greater than 100 min with an average of 127 min. Furthermore, the initial setting times for nearly 80 percent of PLCs were between 130 and 145 min and the reported initial setting times were all well above the minimum requirement of 45 min and well below the maximum limit of 7 h (not shown in figure 31). For comparison purposes, in a survey on 45 commercially available PLCs across the United States in 2022⁽⁵⁾, initial setting time had an average of 113 min and the data ranged from 83 to 165 min showing a larger variation compared to the initial setting time reported for the PLCs tested in this study.

Figure 29. Graph. Chemical characteristics of PLC according to mill test reports. A normal distribution was shown for comparison purposes. (♦ shows the average value for the data.)



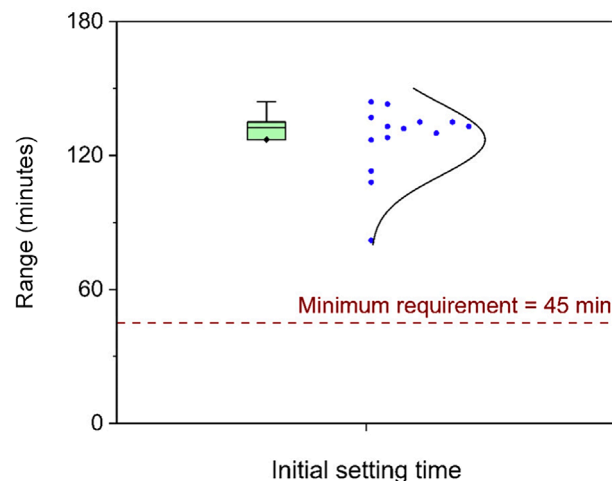
Source: FHWA.

Figure 30. Graph. Physical characteristics of PLC according to mill test reports with (a) showing Blaine fineness, (b) showing mass ratio retained on a No. 325 sieve, and (c) showing the density. A normal distribution was shown for comparison purposes. (♦ Shows the average value for the data.)



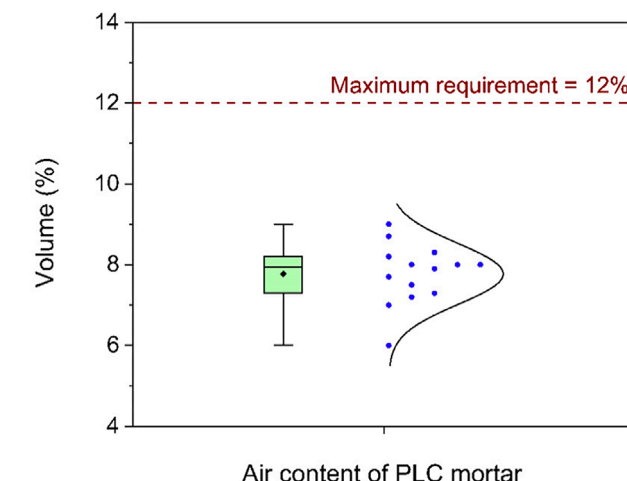
Source: FHWA.

Figure 31. Graph. Initial setting time for the studied PLCs according to mill test reports. A normal distribution was shown for comparison purposes. (♦ shows the average value for the data.)



Source: FHWA.

Figure 32. Graph. Air content in mortars made with the studied PLCs according to mill test reports. A normal distribution was shown for comparison purposes. (♦ shows the average value for the data.)



Source: FHWA.

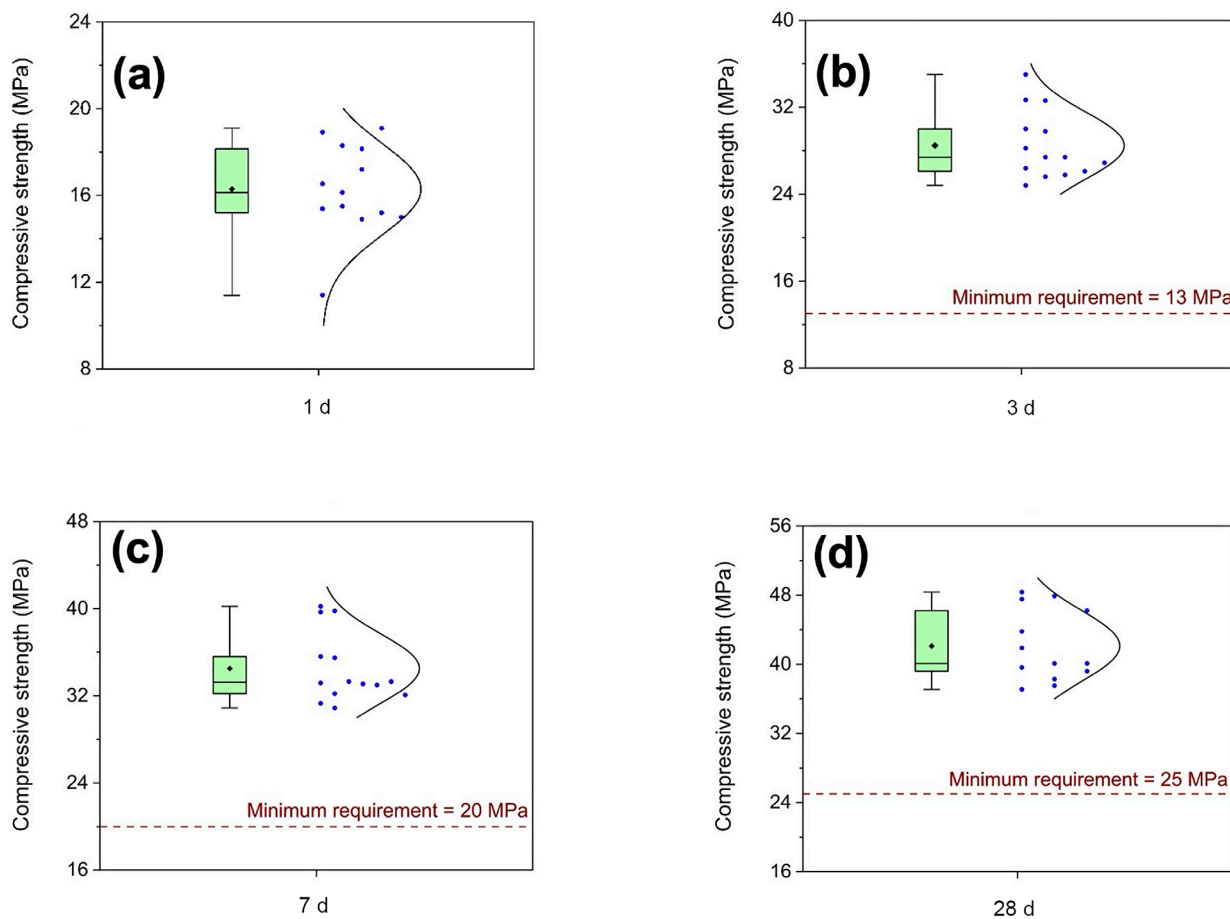
Air content in mortar, although well below the maximum limitation of 12 percent by volume, exhibited high variability, ranging from 6.0 to 9.0 percent by volume, as shown in figure 32. Additionally, compressive strength test results at various curing ages, from 1 d to 28 d, displayed significant variability, as shown in figure 33. According to figure 33, compressive strength of mortar mixtures shows an average of 16.3 ± 2.0 , 28.5 ± 3.0 , 34.5 ± 3.1 , and 42.1 ± 4.0 MPa for 1-d, 3-d, 7-d, and 28-d cured samples, respectively. These values are almost identical to the results from a study on 45 commercially available PLCs in the United States in 2022, showing an average of 16.3 ± 2.3 , 27.5 ± 2.2 , 34.0 ± 2.1 , and 42.3 ± 2.2 MPa for 1-d, 3-d, 7-d, and 28-d cured samples, respectively.⁽⁵⁾ The reported minimum and maximum compressive strength for the PLCs tested in this study were 11.4 and 19.1 MPa, 24.8 and 35.0 MPa, 30.9 and 40.2 MPa, and 37.1 and 48.3 MPa for 1-d, 3-d, 7-d, and 28-d aged mortar samples, respectively. Whereas these values for 45 commercially available PLC in the U.S. market in 2022 were 11.7 and 24.6 MPa, 23.2 and 33.7 MPa, 29.7 and 39.4 MPa, and 36.7 and 46.3 MPa for the corresponding curing ages, respectively.⁽⁵⁾ Comparing these two sets of data indicates

that the compressive strength of commercially produced PLCs in the United States has been consistent over the past few years (2022–2025).

According to the mill test reports, approximately 65 percent of the acquired PLCs were Type IL(10) cements. Type IL(13) was the second most common accounting for 20 percent of the total collected PLC samples. Figure 34 illustrates the distribution of PLC types and their limestone contents based on the type of PLCs.

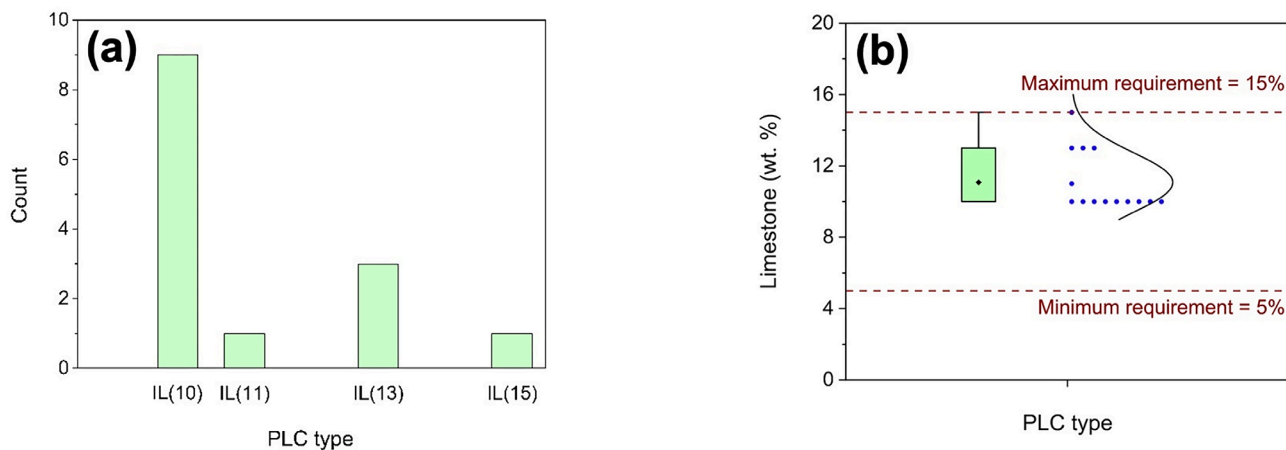
To assess the reliability of the mill test reports for the PLCs used in this study, a linear regression model was applied between the reported data from the manufacturers and the measured data. The correlations from the linear regressions between reported and measured data are provided in figure 35 through figure 39. SO_3 content showed the strongest correlation, followed by LOI and $\text{Na}_2\text{O}_{\text{eq}}$, indicating that the chemical characteristics in the mill test reports are more reliable than the physical characteristics of the PLCs. Figure 38 and figure 39 show no correlation between the reported and measured data for Blaine fineness and density.

Figure 33. Graph. Compressive strength of mortars made with the studied PLCs according to mill test reports at curing ages of (a) 1 d, (b) 3 d, (c) 7 d, and (d) 28 d. A normal distribution was shown for comparison purposes. (♦ shows the average value for the data)



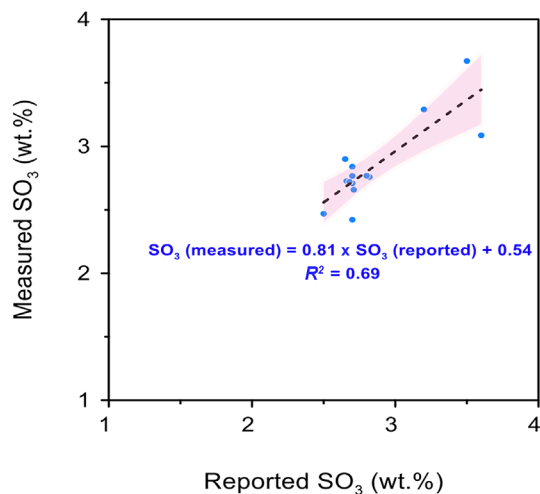
Source: FHWA.

Figure 34. Graph. Type of PLCs employed in this study based on mill test reports with (a) showing the count of PLC types and (b) showing the distribution of PLC limestone weights. A normal distribution was shown for comparison purposes. (♦ shows the average value for the data.)



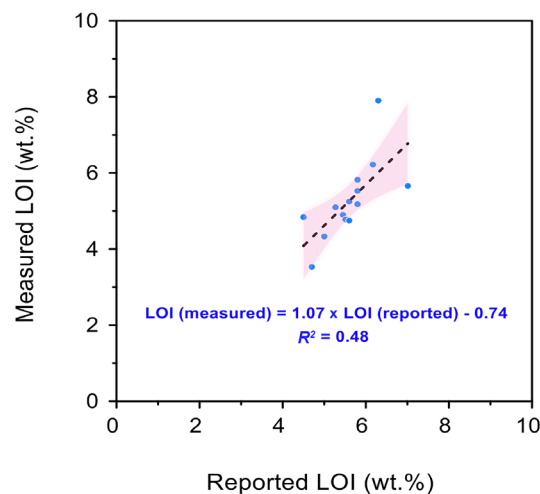
Source: FHWA.

Figure 35. Graph. Relationship between the measured SO_3 content and the SO_3 content reported in mill test reports. The highlighted area shows 95-percent confidence bands and the dashed line is the trendline.



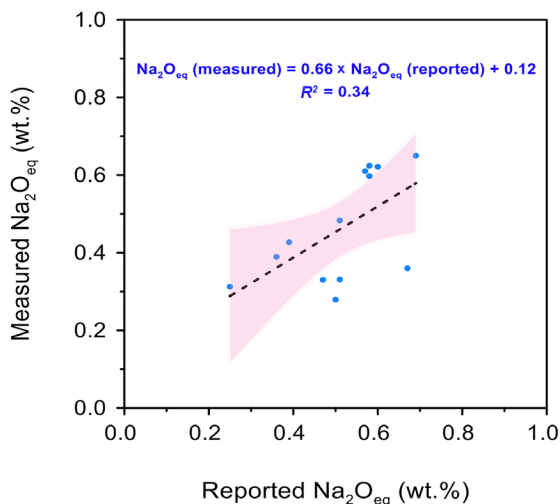
Source: FHWA.

Figure 36. Graph. Relationship between the measured LOI content and the LOI content reported in mill test reports. The highlighted area shows 95-percent confidence bands and the dashed line is the trendline.



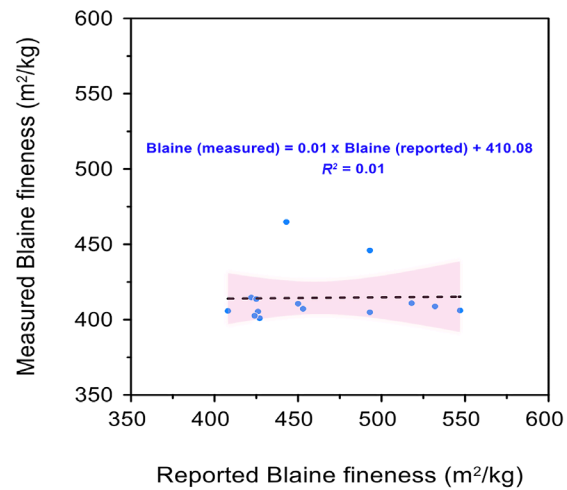
Source: FHWA.

Figure 37. Graph. Relationship between the measured $\text{Na}_2\text{O}_{\text{eq}}$ content and the $\text{Na}_2\text{O}_{\text{eq}}$ content reported in mill test reports. The highlighted area shows 95-percent confidence bands and the dashed line is the trendline.



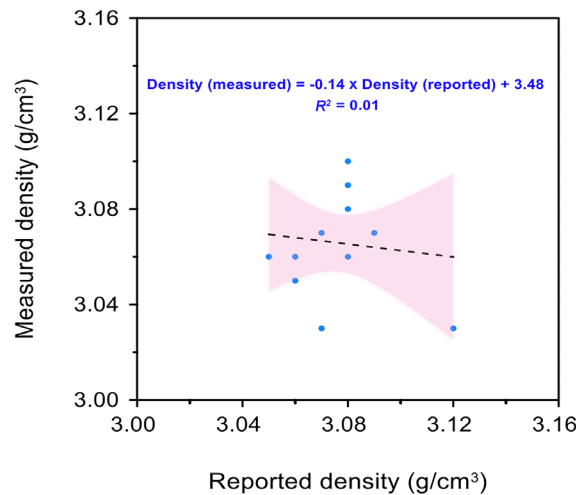
Source: FHWA.

Figure 38. Graph. Relationship between the measured Blaine fineness and Blaine fineness reported in mill test reports. The highlighted area shows 95-percent confidence bands and the dashed line is the trendline.



Source: FHWA.

Figure 39. Graph. Relationship between the measured density and density reported in mill test reports. The highlighted area shows 95-percent confidence bands and the dashed line is the trendline.



Source: FHWA.

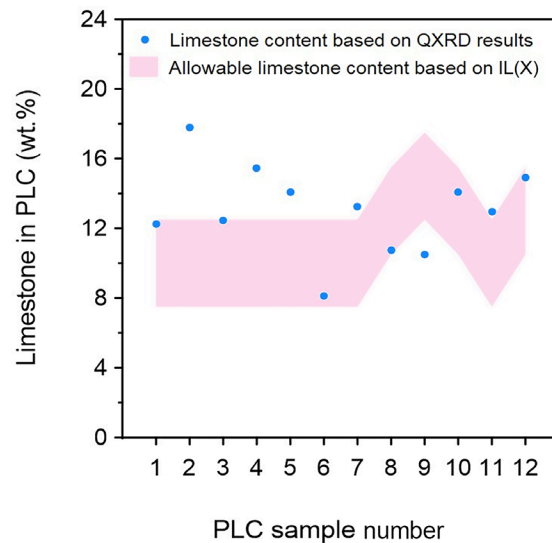
As specified in ASTM C595⁽²⁾ and AASHTO M 240⁽³⁾, a ± 2.5 percent by weight variation in limestone content is permitted for PLC production, resulting in a range of available limestone in PLCs, as indicated by their type, Type IL(X). Figure 40 shows the variation in limestone content in the tested PLCs based on their type mentioned in the mill test reports, represented as $X \pm 2.5$ percent (shaded area), along with the estimated limestone content, which is based on the assumption that dolomitic limestone was used in PLC production, as discussed in the cementitious phase composition section of this document. According to figure 40, even with the allowable range for limestone content, most PLCs had equal to or higher limestone content than the maximum limitation based on the PLC type. This finding indicates significant variation in limestone content during the PLC production process.

9. SUMMARY

The results of this study's data analysis indicate the following conclusions:

- Physical and chemical characteristics:
 - Most of the PLCs tested in this study (15 out of 18) exhibited Blaine fineness values ranging from 400 to 415 m^2/kg .
 - The finer portion of the PLC samples exhibited narrower variability, with $D_{(10)}$ showing smaller variations than $D_{(50)}$ and $D_{(50)}$ displaying smaller variations than $D_{(90)}$.
 - All PLCs tested in this study exhibited three distinct humps in their particle size distribution, occurring within the ranges of 0.1–1.0 μm , 1.0–10.0 μm , and 10.0–50.0 μm , indicating the presence of three distinct particle size groups.
 - Most of the PLCs tested in this study (15 out of 18) had densities ranging from 3.05 to 3.10 g/cm^3 .
 - Several PLCs (7 out of 18) exceeded the 3.0 percent by weight threshold for SO_3 ; however, according to their technical data sheets, they complied with the requirements of ASTM C1038.⁽²⁹⁾
 - The mass ratios of the calcium silicates, alite (C_3S) and C_2S , ranged from 49.4 to 64.9 percent and 5.0 to 10.7 percent, respectively, for the tested PLCs. The mass ratio ranges for the other main clinker phases were 3.4 to 10.7 percent for aluminate (C_3A) and 6.7 to 12.1 percent for C_4AF .

Figure 40. Graph. Variation in limestone content based on the PLC type allowable variation (± 2.5 percent by weight) and the estimated dolomitic limestone in the tested PLCs. Shaded area shows allowable limestone content based on Type IL(X) from mill test reports.



Source: FHWA.

- $\text{Ca}(\text{OH})_2$ was observed in all the tested PLCs, indicating slight prehydration during handling from the plant to the lab or job site.
- Calcite was the only polymorph of CaCO_3 identified in the PLC samples through X ray diffraction analysis, with its mass ratio ranging from 5 to 17 percent based on TGA and QXRD calculations.
- Given the negligible quartz content and the presence of dolomite, the most likely limestone rock used as feedstock for producing the studied PLCs was dolomitic limestone. Based on this assumption, the limestone mass content in the studied PLCs ranges from 7 to 18 percent.
- For the tested PLCs, the LOI ranged from approximately 3 to 8 percent by weight. CaCO_3 content in PLC can be estimated by measuring the LOI, following the procedures outlined in ASTM C114.⁽²⁸⁾
- Reactivity:
 - Increasing w/c from 0.40 to 0.50 increases the reactivity of PLC, as shown by a greater total heat release in the first 7 d and a higher H_u .

- The influence of the w/c on early-age reactivity becomes more pronounced at later ages, particularly at 3 and 7 d, with H_u exhibiting the strongest correlation, emphasizing the significant impact of water availability on later-age reactivity. Additionally, H_u data showed greater variability at a higher w/c (0.50 versus 0.40), underscoring the crucial role of the w/c in achieving a higher degree of hydration in PLC systems.
- Among the physical characteristics of PLC, variability in particle size significantly impacts its reactivity, especially during the first day of hydration.
- Variation in Blaine fineness had an insignificant effect on the hydration progress of the studied PLCs.
- The chemical composition of PLC significantly affects its reactivity. Al_2O_3 , SO_3 , MgO , and K_2O have a greater influence on the 1-d reactivity of PLC, while Na_2O has a more pronounced impact on its reactivity at 3 and 7 d. However, the oxide composition of PLCs did not significantly affect their maximum degree of hydration, as reflected in the H_u data.
- Alite had a higher direct effect on hydration progress during the first 3 d of reaction. In contrast, the aluminate phase showed an inverse effect on the 1-d reactivity of the studied PLCs. The combination of alite and aluminate had a greater influence on 3-d and 7-d reactivity.
- The addition of calcium sulfates (gypsum and bassanite) to PLC further enhances alite and aluminate effectiveness in promoting hydration, highlighting the importance of sulfate adjustment in PLC systems to achieve a higher degree of reaction during the early age. Higher reactivity is particularly crucial for developing high early-strength concretes using PLC.
- The combination of calcite and alite proved to be more effective in 1-d hydration, while the incorporation of aluminate and sulfate with alite and calcite enhanced their effect on 3-d and 7-d hydration for the studied PLCs, emphasizing the importance of the aluminate and sulfate combination in improving PLC hydration during the early age.
- The initial and final setting times for the studied PLCs (w/c = 0.40) ranged from 150 to 230 min and 240 to 450 min, respectively. The final setting times exhibited more variability than the initial setting time data for the studied PLCs.

- Batch variability:

- Batch-to-batch variability revealed minimal variation in the early-age reactivity (up to 7 d) of the four Type IL(10) from the same plant.
- Insignificant changes in early-age hydration among different batches of PLC can be attributed to the consistent values of key factors influencing early-age reactivity, including average particle size (up to 25 percent variation), major oxides such as Al_2O_3 , SiO_2 , CaO , SO_3 , and Fe_2O_3 (up to 8 percent variation), and alite (up to 10 percent variation). In addition, among the various batches, the final setting time exhibited greater variation than the initial setting time.

- Mill test results variability:

- Analysis of the data obtained from mill test reports showed high variability in chemical, physical, and performance characteristics of the tested PLCs.
- A stronger correlation was found between the reported and measured chemical characteristics as compared to lack of correlation between physical characteristics data.
- High variability was found in limestone content in the tested PLCs according to their type.

10. REFERENCES

1. Federal Highway Administration. 2023. *Portland Limestone Cement*. Publication No. FHWA-HRT-23-104. Washington, DC: Federal Highway Administration.
2. ASTM International. 2021. *Standard Specification for Blended Hydraulic Cements*. ASTM C595/C595M. West Conshohocken, PA: ASTM International. https://store.astm.org/c0595_c0595m-21.html, last accessed June 16, 2025.
3. AASHTO. 2021. *Standard Specification for Blended Hydraulic Cement*. AASHTO M 240M/M 240. Washington, DC: American Association of State Highway and Transportation Officials. https://store.accuristech.com/standards/aashto-m-240m-m-240-23?product_id=2573615&srsltid=AfmBOoqszmWwGL1eu0Ohi7FjFh2nxCiJhyVXZAeFEibdhDK_SIWnI8qD, last accessed June 16, 2025.
4. U.S. Geological Survey. 2024. “Mineral Industry Surveys” (web page). <https://www.usgs.gov/centers/national-minerals-information-center/mineral-industry-surveys>, last accessed September 25, 2024.

5. Farny, J. 2025. *Chemical and Physical Characteristics of US Hydraulic Cements*: 2022. Report No. SN3354. Washington, DC: Portland Cement Association. <https://doi.org/10.70909/pca.2025.SN3354>, last accessed June 16, 2025.
6. Klinger, J., K. A. MacDonald, J. A. Holland, S. M. Tarr, B. A. Garnant, and B. A. Suprenant. 2024. “ACI-ASCC Survey on Portland-Limestone Cement Concrete.” *Concrete International* 46, no. 2: 27–36.
7. Kurtis, K. E., L. F. Kahn, A. Shalan, B. Zaribaf, and E. Nadelman. 2017. *Assessment of Limestone Blended Cements for Transportation Applications*. Report No. FHWA-GA-17-13-09. Atlanta, GA: Georgia Department of Transportation.
8. Bharadwaj, K., O. B. Isgor, and W. J. Weiss. 2022. “Supplementary Cementitious Materials in Portland-Limestone Cements.” *ACI Materials Journal* 119, no. 2: 141–154. <https://doi.org/10.14359/51734356>, last accessed June 16, 2025.
9. Campagiorni, L., M. Tonelli, and F. Ridi. 2025. “Synergistic Effect of Limestone and Supplementary Cementitious Materials in Ternary Blended Cements.” *Current Opinion in Colloid & Interface Science* 75, no. 101885. <https://doi.org/10.1016/j.cocis.2024.101885>, last accessed June 16, 2025.
10. Chopperla, K. S. T., J. A. Smith, and J. H. Ideker. 2022. “The Efficacy of Portland-Limestone Cements with Supplementary Cementitious Materials to Prevent Alkali-Silica Reaction.” *Cement* 8: 100031. <https://doi.org/10.1016/j.cement.2022.100031>, last accessed June 16, 2025.
11. Tennis, P. D., D. A. Thomas, W. J. Weiss, J. A. Farny, and E. R. Giannini. 2024. *State-of-the-Art Report on Use of Limestone in Cements at Levels of up to 15 Percent*. Report No. PCA R&D SN3148. Washington, DC: Portland Cement Association.
12. Thomas, M. D. A., D. Hooton, K. Cail, B. A. Smith, J. de Wal, and K. G. Kazanis. 2010. “Field Trials of Concretes Produced with Portland Limestone Cement.” *Concrete International* 32, no. 1: 35–41.
13. Hansen, B. S., I. L. Howard, J. Shannon, T. Cost, and W. M. Wilson. 2020. “Portland-Limestone Cement Fineness Effects on Concrete Properties.” *Materials Journal* 117, no. 2. <https://doi.org/10.14359/51720301>, last accessed June 16, 2025.
14. ASTM International. 2020. *Standard Test Method for Slump of Hydraulic-Cement Concrete*. ASTM C143. West Conshohocken, PA: ASTM International.
15. Barrett, T. J., H. Sun, T. Nantung, and W. J. Weiss. 2014. “Performance of Portland Limestone Cements.” *Transportation Research Record* 2441, no 1: 112–120. <https://doi.org/10.3141/2441-15>, last accessed June 16, 2025.
16. ASTM International. 2022. *Standard Test Method for Electrical Indication of Concrete’s Ability to Resist Chloride Ion Penetration*. ASTM C1202. West Conshohocken, PA: ASTM International.
17. AASHTO. 2023. *Standard Method of Test for Electrical Indication of Concrete’s Ability to Resist Chloride Ion Penetration*. AASHTO T 277. Washington, DC: American Association of State Highway and Transportation Officials.
18. ASTM International. 2017. *Standard Test Method for Effectiveness of Pozzolans or Ground Blast-Furnace Slag in Preventing Excessive Expansion of Concrete Due to the Alkali-Silica Reaction*. ASTM C441. West Conshohocken, PA: ASTM International.
19. MapChart. 2025. “MapChart” (website). <https://mapchart.net>, last accessed March 20, 2025.
20. Kosmatka, S. H., M. L. Wilson. 2011. *Design and Control of Concrete Mixtures, 15th Edition*. Skokie, IL: Portland Cement Association.
21. ASTM International. 2020. *Standard Test Method for Compressive Strength of Hydraulic Cement Mortars (Using 2-in. or [50-Mm] Cube Specimens)*. ASTM C109. West Conshohocken, PA: ASTM International.
22. ASTM International. 2024. *Standard Test Methods for Fineness of Hydraulic Cement by Air-Permeability Apparatus*. ASTM C204. West Conshohocken, PA: ASTM International.
23. AASHTO. 2020. *Standard Method of Test for Fineness of Hydraulic Cement by Air Permeability Apparatus*. AASHTO T 153. Washington, DC: American Association of State Highway and Transportation Officials.
24. Arvaniti, E. C., M. C. G. Juenger, S. A. Bernal, J. Duchesne, L. Courard, S. Leroy, J. L. Provis, A. Klemm, N. De Belie. 2015. “Physical Characterization Methods for Supplementary Cementitious Materials.” *Materials and Structures* 48, no. 11: 3675–3686. <https://doi.org/10.1617/s11527-014-0430-4>.

25. ASTM International. 2023. *Standard Test Method for Density of Hydraulic Cement*. ASTM C188. West Conshohocken, PA: ASTM International.

26. Helsel, M. A., C. F. Ferraris, and D. Bentz. 2016. "Comparative Study of Methods to Measure the Density of Cementitious Powders." *Journal of Testing and Evaluation* 44, no. 6: 2147–2154. <https://doi.org/10.1520/JTE20150148>, last accessed June 16, 2025.

27. ASTM International. 2022. *Standard Specification for Portland Cement*. ASTM C150/C150M-12. West Conshohocken, PA: ASTM International.

28. ASTM International. 2022. *Standard Test Methods for Chemical Analysis of Hydraulic Cement*. ASTM C114. West Conshohocken, PA: ASTM International.

29. ASTM International. 2024. *Standard Test Method for Expansion of Hydraulic Cementitious Material Mortar Bars Stored in Water*. ASTM C1038. West Conshohocken, PA: ASTM International.

30. Rietveld, H. M. 1969. "A Profile Refinement Method for Nuclear and Magnetic Structures." *Journal of Applied Crystallography* 2, no. 2: 65–71. <https://doi.org/10.1107/S0021889869006558>, last accessed June 16, 2025.

31. ASTM International. 2018. *Standard Test Method for Determination of the Proportion of Phases in Portland Cement and Portland-Cement Clinker Using X-Ray Powder Diffraction Analysis*. ASTM C1365. West Conshohocken, PA: ASTM International.

32. Nadelman, E. I. 2016. *Hydration and Microstructural Development of Portland Limestone Cement-Based Materials* (Doctoral Dissertation). Atlanta, GA: Georgia Institute of Technology.

33. ASTM International. 2017. *Standard Test Method for Measurement of Heat of Hydration of Hydraulic Cementitious Materials Using Isothermal Conduction Calorimetry*. ASTM C1702. West Conshohocken, PA: ASTM International.

34. Snellings, R., H. Kazemi-Kamyab, P. Nielsen, L. Van Den Abeele. 2021. "Classification and Milling Increase Fly Ash Pozzolanic Reactivity." *Front. Built Environ.* 7: 670996. <https://doi.org/10.3389/fbuil.2021.670996>, last accessed June 16, 2025.

35. Spearman, R. 2008. "Spearman Rank Correlation Coefficient." In *The Concise Encyclopedia of Statistics*. Springer: New York, NY, pp. 502–505. https://doi.org/10.1007/978-0-387-32833-1_379, last accessed June 16, 2025.

36. Maier, M., S. Scherb, and K. Thienel. 2023. "Sulfate Consumption During the Hydration of Alite and Its Influence by SCMs." Paper presented at the *21st ibausil International Conference on Building Materials*. Weimar, Germany: Institut an der Bauhaus-Universität Weimar. <https://doi.org/10.1002/cepa.2885>, last accessed June 16, 2025.

37. Bergold, S. T., F. Goetz-Neunhoeffer, and J. Neubauer. 2017. "Interaction of Silicate and Aluminate Reaction in a Synthetic Cement System: Implications for the Process of Alite Hydration." *Cement and Concrete Research* 93: 32–44. <https://doi.org/10.1016/j.cemconres.2016.12.006>, last accessed June 16, 2025.

38. ASTM International. 2021. *Standard Test Methods for Time of Setting of Hydraulic Cement by Vicat Needle*. ASTM C191. West Conshohocken, PA: ASTM International.

39. Song, Q., J. Su, J. Nie, H. Li, Y. Hu, Y. Chen, R. Li, and Y. Deng. 2021. "The Occurrence of MgO and Its Influence on Properties of Clinker and Cement: A Review." *Construction and Building Materials* 293: 123494. <https://doi.org/10.1016/j.conbuildmat.2021.123494>, last accessed June 16, 2025.

40. Federal Highway Administration. *Alkali-Silica Reaction Mechanisms and Detection: An Advanced Understanding*. Report No. FHWA-HRT-14-079. Washington, DC: Federal Highway Administration.

41. Kabir, H., R.D. Hooton, and N.J. Popoff. 2020. "Evaluation of Cement Soundness Using the ASTM C151 Autoclave Expansion Test." *Cement and Concrete Research* 136: 106159. <https://doi.org/10.1016/j.cemconres.2020.106159>, last accessed June 16, 2025.

42. Montgomery, D. C. 2019. *Introduction to Statistical Quality Control, 8th Edition*. Hoboken, NJ: John Wiley & Sons, Inc.

43. ASTM International. 2025. *Standard Test Method for Fineness of Hydraulic Cement by the 45- μm (No. 325) Sieve*. ASTM C430. West Conshohocken, PA: ASTM International.
44. ASTM International. 2025. *Standard Test Method for Fineness of Hydraulic Cement by Air Jet Sieving at 45- μm (No. 325)*. ASTM C1891. West Conshohocken, PA: ASTM International.
45. ASTM International. 2020. *Standard Test Method for Air Content of Hydraulic Cement Mortar*. ASTM C185. West Conshohocken, PA: ASTM International.

Researchers—This study was conducted by Payam Hosseini of the Turner-Fairbank Highway Research Center Concrete Laboratory under contract number 693JJ323D000008, Michelle Cooper of the FHWA Office of Infrastructure Research and Development, and Scott Muzenski of the Turner-Fairbank Highway Research Center Concrete Laboratory under contract number 693JJ323D000008.

Distribution—This TechNote is being distributed according to a standard distribution. Direct distribution is being made to the FHWA divisions.

Availability—This TechNote may be obtained at <https://highways.dot.gov/research>.

Key Words—Portland limestone cement, concrete, PLC, variability, cement, limestone.

Notice—This document is disseminated under the sponsorship of the U.S. Department of Transportation (USDOT) in the interest of information exchange. The U.S. Government assumes no liability for the use of the information contained in this document.

Non-Binding Contents—Except for the statutes and regulations cited, the contents of this document do not have the force and effect of law and are not meant to bind the States or the public in any way. This document is intended only to provide information regarding existing requirements under the law or agency policies.

Quality Assurance Statement—The Federal Highway Administration (FHWA) provides high quality information to serve Government, industry, and the public in a manner that promotes public understanding. Standards and policies are used to ensure and maximize the quality, objectivity, utility, and integrity of its information. FHWA periodically reviews quality issues and adjusts its programs and processes to ensure continuous quality improvement.

Disclaimer for Product Names and Manufacturers—The U.S. Government does not endorse products or manufacturers. Trademarks or manufacturers' names appear in this document only because they are considered essential to the objective of the document. They are included for informational purposes only and are not intended to reflect a preference, approval, or endorsement of any one product or entity.